

Spectroscopic characteristics of the cyanomethyl anion and its deuterated derivatives

Liton Majumdar¹, Ankan Das¹, Sandip K. Chakrabarti^{2,1}

¹ Indian Centre for Space Physics, Chalantika 43, Garia Station Rd., Kolkata, 700084, India

e-mail: ankan@csp.res.in, liton@csp.res.in

² S. N. Bose National Centre for Basic Sciences, Salt Lake, Kolkata 700098, India

e-mail: chakraba@bose.res.in

Received ; accepted

ABSTRACT

Context. It has long been suggested that CH_2CN^- (cyanomethyl anion) might be a carrier of one of the many poorly characterized diffuse interstellar bands. In this paper, our aim is to study various forms (ionic, neutral & deuterated isotopomer) of CH_2CN (cyanomethyl radical) in the interstellar medium.

Aims. Aim of this paper is to predict spectroscopic characteristics of various forms of CH_2CN and its deuterated derivatives. Moreover, we would like to model the interstellar chemistry for making predictions for the column densities of such species around dark cloud conditions.

Methods. We have performed detailed quantum chemical simulations to present the spectral properties (infrared, electronic & rotational) of various forms of the cyanomethyl radical. Moller-Plesset perturbation theory along with the triple-zeta correlation-consistent basis set is used to obtain different spectroscopic constants of CH_2CN^- , CHDCN^- and CD_2CN^- in the gas phase which are essential to predict rotational spectra of these species. Depending on the total number of electrons, there exist several allowed spin states for various forms of the cyanomethyl radical. We performed quantum chemical calculation to find out energetically the most stable spin states for these species. We have computed IR and electronic absorption spectra for different forms of CH_2CN . Moreover, we have also implemented a large gas-grain chemical network to predict the column densities of various forms of the cyanomethyl radical and its related species. In order to mimic physical conditions around a dense cloud region, the variation of the visual extinction parameters are considered with respect to the hydrogen number density of the simulated cloud.

Results. Our quantum chemical calculation reveals that the singlet spin state is the most stable form of cyanomethyl anion and its deuterated forms. For the confirmation of the detection of the cyanomethyl anion and its two deuterated forms, namely, CHDCN^- and CD_2CN^- , we present the rotational spectral information of these species in the Appendix. Our chemical model predicts that the deuterated forms of cyanomethyl radicals (specially the anions) are also reasonably abundant around the dense region of the molecular cloud.

Key words. Interstellar Medium, Astrochemistry, Molecular cloud, Star formation

1. Introduction

Over the past years, several works have been carried out to investigate the formation of complex molecules in and around cold interstellar clouds (Hasegawa and Herbst 1993; Hasegawa, Herbst and Leung 1992; Majumdar et al. 2012, Majumdar et al. 2013, Das et al. 2013a). Till date, more than 170 molecules have been observed in Interstellar Mediums (ISMs) or circumstellar shells. It is now well known that in order to model the formation of complex molecules in ISMs, the interstellar grain chemistry has to be an integral part of the chemical evolutionary path (Stantcheva, Shematovich and Herbst 2002, Chakrabarti et al. 2006a,b; Das et al. 2008b, Das, Acharyya & Chakrabarti, 2010; Das & Chakrabarti, 2011; Cuppen & Herbst, 2007; Cuppen et al. 2009).

One of the stumbling blocks in spectroscopy in astronomical context is the lack of adequate knowledge of the origin of unidentified diffuse interstellar bands (DIBs). These DIBs are basically a series of absorption lines that are observed toward just about every star in our galaxy that has interstellar material in front of it. Herbig (1995) and Sarre (2006) reviewed the very long-standing problem of the diffuse interstellar bands. They pointed out that some organic molecules could be the possible candidates for more than 300 DIBs in the ISM. According to Sarre (2000), some (possibly many) of the DIBs are due to electronic transitions between the ground and the dipole bound states of negatively charged polar molecules or small polar grains. Sarre (2000) also first pointed out that CH_2CN^- might be a carrier of the DIBs. A follow up study by Cordiner & Sarre (2007) explored the possibility of CH_2CN^- as a possible carrier of the narrow DIB at $8037 \pm 0.15 \text{ \AA}$.

The cyanomethyl radical (CH_2CN) is the simplest cyanide derivative of the methyl radical (CH_3). Due to the presence of a cyano group in the molecule, a dipole moment is generated which makes it possible to search for the CH_2CN radical by electric-dipole allowed microwave transitions. According to Herbst (2001), an appreciable amount of CH_3 radical is expected in the diffuse and dense molecular clouds. The first detection of CH_2CN was reported by Irvine et al. (1988), in two of the best characterized molecular clouds, namely, TMC-1 and Sgr B2. Their work was based on the observations performed using the decommissioned 14m antenna at the Five College Radio Astronomy Observatory, the 43m antenna at NRAO's Green Bank facility, the 20m antenna at Onsala Space Observatory, and the 45m antenna at Nobeyama Radio Observatory. A few years ago, the observed spectra was verified experimentally in the laboratory by Ozeki et al. (2004), using a Fourier-transform microwave spectrometer in combination with a pulsed-discharge nozzle. The first detection of CH_2CN in IRC +10216 was reported by Agundez et al. (2008).

Lykke et al. (1987) employed the auto-detachment spectroscopy technique to study the dynamics of CH_2CN^- and one of its deuterated isotopomers, namely, CD_2CN^- . In their work,

dynamics of the auto-detachment process was studied and various mechanisms for detachment were described. Cordiner & Sarre (2007) used the rotational constants obtained by Lykke et al. (1987) to compute the absorption spectrum arising from the ${}^1B_1 - \tilde{X}^1 A'$ transition of CH_2CN^- for CH_2CN^- in equilibrium with CMB at 2.74K. According to their calculation, if CH_2CN^- is present in the ISM with an ortho to para abundance ratio of 3:1, ${}^1B_1 - \tilde{X}^1 A'$ transitions having $K_a'' = 1$ would produce strong spectral features at 8024.8A° and 8049.6A° . However, these features are absent in the interstellar spectra. Hence, according to them though $\lambda 8037$ DIB and transition of CH_2CN^- is consistent, this could not be treated as granted. Further study regarding the CH_2CN^- is essential for making such strong assignments. Fortenberry & Crawford (2011a) carried out quantum chemical calculations for the prediction of new dipole-bound singlet states for anions of interstellar interest. Fortenberry, Crawford & Lee (2013) used quartic force fields and second order vibrational perturbation theory to calculate the appropriate spectroscopic constants and fundamental vibrational frequencies for $\tilde{X}^1 A'$ CH_2CN^- to facilitate its confirmed detection.

According to Park and Woon, (2006), ions embedded in icy grain mantles are thought to account for various observed infrared spectroscopic features, particularly in certain young stellar objects like W33A. Observations of different interstellar molecules (CH_3OH , HCOOH , NH_3 , H_2O , CO , CO_2 , CH_4 , H_2CO , OCS etc.) by Gibb et al. (2000), anions (OCN^- , HCOO^-) by Soifer et al. (1979) and Schutte et al. (1997, 1999), cations (HCO^+ , NH_4^+) by Schutte & Greenberg (1997), Demyk et al. (1998), Hudson et al. (2001), Novozamsky et al. (2001) motivated us to consider the spectroscopy of different forms (neutral, cationic, anionic) of CH_2CN embedded in icy grain mantles. According to Park and Woon, (2006), quantum chemical approach along with a continuum model is well suited for modeling the spectroscopic properties of molecules and ions embedded within amorphous ice matrices. Inspired by these studies, we performed a detail spectroscopy as well as astrochemical modeling of different forms of CH_2CN . We expect that our study would throw lights on the possibility of finding other forms of CH_2CN in and around ISMs.

The plan of this paper is the following. In Section 2, method and computational details for the purpose of spectroscopy of CH_2CN and its related molecules are discussed. Different computational results are presented in Section 3. In Section 4, we draw our conclusion. In Appendix A, we discuss the chemical modeling and results. Moreover, in the Appendix B, we have included four Tables for presenting different vibrational (Table B1) and rotational transitions (Table B2, B3 & B4).

2. Methods and Computational Details

2.1. Quantum chemical simulation & spectroscopy

Recent work by Huang & Lee (2008) suggests that the quantum chemical computational tools could be very useful to obtain rotational constants often within an accuracy of 20 MHz (especially

for the B-type and C-type constants). Vibrational frequencies accurate to 5 cm^{-1} or better could be obtained from the quantum chemical calculations (Huang & Lee 2008, 2009, 2011; Huang et al. 2011; Inostroza et al. 2011; Fortenberry & Crawford 2011a, 2011b, 2011c; Fortenberry et al. 2012a, 2012b; Fortenberry, Crawford & Lee, 2013). Motivated by these works, we perform a detailed quantum chemical simulation to report various spectral aspects of different forms of CH_2CN molecule in the vibrational (harmonic), electronic and rotational mode.

All the computations on neutral CH_2CN are performed by using spin-unrestricted (UHF) wave functions, while computations of the closed-shell anions used spin-restricted (RHF) wave functions. First, the geometries of the neutral and ionic forms of CH_2CN are optimized at Becke three-parameter Exchange and Lee, Yang and Parr correlation functional (B3LYP) with 6-311++G as the basis set. B3LYP is the most popular DFT model. This method is termed as a hybrid method, because it uses corrections for both gradient and exchange correlations. Becke Three Parameter Hybrid Functional forms were devised by Becke in (1993) along with the non-local correlation provided by LYP (Lee, Yang & Parr 1988). Dipole moments of all of these species are computed by using the same level of theory. For the computation of dipole moments, we have considered the center of mass to be our standard origin in the Gaussian 09W program (Frisch et al. 2009). Gas phase vibrational frequencies of these species are obtained from the minimum energy structure at the same level of theory. Our computed vibrational frequencies are harmonic in nature since the Gaussian 09W program computes these frequencies based on the harmonic oscillator approximation. In order to find out the harmonic vibrational frequencies of these species in the ice phase, we have also optimized these geometries in B3LYP/6-311++G level using the SCRF method. The SCRF method in Gaussian 09W program is used to perform calculations in presence of a solvent by placing the solute in a cavity within a solvent reaction field. The Polarizable Continuum Model (PCM) using the integral equation formalism variant (IEFPCM) is the default SCRF method. This method creates the solute cavity via a set of overlapping spheres. It was initially devised by Tomasi and co-workers and Pascual-Ahuir and co-workers (Tomasi et al. 2002; Tomasi, Mennucci & Cammi 2005; Tomasi, Mennucci & Cancès 1999, Pascual-Ahuir, Silla & Tun 1994). The electronic absorption spectra of these species are also obtained using the higher order method (EOM-CCSD) with the basis set aug-cc-pVDZ. This method use coupled cluster for the description of excited states using the equation of motion approach. Depending on the total number of electrons of a species, we vary the spin multiplicities to locate the most reasonable spin state. In order to get more accurate information about the rotational spectral parameters (rotational & distortional constants), we have used MP2/aug-cc-pVTZ level of theory in the symmetrically as well as asymmetrically reduced Hamiltonian. Rotational motion of a molecule in Gaussian 09W program commonly starts from the rigid rotor model which assumes that the molecule is rigid. For our calculation, we have to know the structure of the molecule and from that we could get the moment of inertia which could then utilized to obtain the eigen values. Generally, this requires a very good estimation of the structure and optimization of a molecule. In an earlier paper (Das et al. 2013), we carried out a similar type of calculation for

HCOCN, where we implemented MP2/aug-cc-pVTZ level of theory and showed that this level of theory produced results which were in good agreement with the experiment. For the computation of vibrationally averaged structures, the corrections for the interactions between rotation and vibration are important. We have computed these vibrational-rotational coupling by Gaussian 09W program. Further corrections for vibrational averaging and anharmonic corrections to the vibration are also implemented by using Gaussian 09W program. These rotational and distortional constants are required to predict the spectrum of a particular species. Herb Pickett's SPCAT program (Pickett, 1991) was designed in such a way that one would get the spectral information by putting the rotational and distortional constants and other relevant parameters according to the prescribed format. In our calculations, rotational and distortional constants are computed from the Gaussian 09W program. These values are then inserted into the SPCAT program to obtain the spectral information of CH_2CN^- , CHDCN^- and CD_2CN^- .

3. Results and Discussion

3.1. Chemical parameters

The way the energy of a molecular system varies with small changes in its structure is specified by its potential energy surface. In this work, the geometry optimization of different forms of CH_2CN (neutral, ionic and its isotopomers) has been performed to locate the minima on the potential energy surface, thereby predicting the equilibrium structure of these molecules. At the minima, the first derivative of the energy (i.e., the energy gradient) is zero and thus the forces are also zero. It is customary to know energetically the most stable form of CH_2CN that can exist in and around the ISM. In Table 1, we provide the relative energies of the different spin states of the gas/ice phase CH_2CN , CH_2CN^+ and CH_2CN^- in eV unit and their dipole moments in Debye unit. Dipole moments of all the species are computed by considering the center of mass as our standard origin. For the neutral CH_2CN , the total number of electrons are 21. Because it is an odd number, the allowed spin states are doublet, quartet, sextet etc. By performing the geometry optimization and energy calculation at B3LYP/6-311++G level of theory, we found that the doublet spin state of neutral CH_2CN is most stable. Relative energies of the quartet and sextet spin states of CH_2CN with respect to its minimum energy spin state (doublet) are found to be 4.08 eV and 8.16 eV respectively. The mono-cationic form of CH_2CN (CH_2CN^+) is an even electron system which corresponds to the fact that it has the singlet, triplet, quintet etc. as the allowed spin states. Among these allowed spin states, the singlet spin state is found to be the most stable spin state for CH_2CN^+ . Relative energies of the triplet and quintet spin states of CH_2CN^+ with respect to its minimum energy spin state (singlet) are found to be 1.94 eV and 5.47 eV respectively. The cyanomethyl anion also has an even electron system having singlet, triplet, quintet etc. as the allowed spin states. The singlet spin state of CH_2CN^- is found to be most stable spin state. Relative energies of the triplet and quintet spin states of CH_2CN^- with respect to its minimum energy spin state (triplet) are found to be 2.06 eV and 6.35 eV respectively. In

Table 1. Relative energies (eV) of different forms of CH₂CN (neutral, cationic & anionic) in the gas phase and the ice phase along with their dipole moments.

Species	Spin State	Relative energy in gas phase (in eV)	Dipole moments in gas phase (in Debye)	Relative energy in ice phase (in eV)	Dipole moments in gas phase (in Debye)
CH ₂ CN	doublet	0	3.5974	0	4.6355
	quartet	4.08	2.4705	4.15	3.3207
	sextet	8.16	1.5430	8.28	1.8471
CH ₂ CN ⁺	singlet	0	5.305	0	6.606
	triplet	1.94	3.802	2.08	4.474
	quintet	5.47	3.653	5.63	4.213
CH ₂ CN ⁻	singlet	0	1.212	0	2.469
	triplet	2.06	6.712	3.17	3.183
	quintet	6.35	6.5460	6.52	2.8671

Table 1, the relative energies of different spin states of neutral CH₂CN, CH₂CN⁺ and CH₂CN⁻ are shown along with their respective dipole moments.

These molecules could also be trapped into the interstellar ice. So it is also necessary to identify the most stable configuration of the various forms of CH₂CN in the interstellar grain. For this purpose, we have considered the self-consistent reaction field method which considers the solvent (ice) as a continuum of uniform dielectric constant and the solute (different forms of CH₂CN) is placed into a cavity within the solvent. In the ice phase, it has been found that the doublet CH₂CN (dipole moment= 4.6355 Debye), singlet CH₂CN⁺ (dipole moment= 6.606 Debye) and singlet CH₂CN⁻ (dipole moment= 2.469 Debye) are the most stable configurations in the ice phase. Among the deuterated forms, doublet CD₂CN, singlet CD₂CN⁺, singlet CD₂CN⁻, doublet CHDCN, singlet CHDCN⁺, singlet CHDCN⁻, are the most stable configurations in the ice phase.

3.2. Astronomical spectroscopy

3.2.1. Vibrational spectroscopy

In order to study the spectral properties (vibrational) for various forms of CH₂CN, we need to compute the infrared peak positions with their absorbance in the gas phase and in other astrophysical environments. As discussed in Sec 3.1, depending on the total electron content of the system, the spin multiplicity varies. In the present work, we have considered that the neutral, mono-cationic and mono-anionic forms of CH₂CN are possible in the ISM. For each of this state, we considered three different spin states.

In Table B1, we present vibrational frequencies (harmonic) of CH₂CN with its different charge and spin states for the gas phase and the ice phase. Observational evidences suggest that ice could be mixed in nature. Major contributor of interstellar ice is H₂O but carbon monoxide and methanol are also contributing significantly (Keane et al. 2001; Das & Chakrabarti, 2011). Since H₂O is the major constituent (> 70%) of the interstellar ice, we are considering only the water ice for our simulation purpose. For the pure water ice, Gaussian 09W uses a dielectric con-

stant of ~ 78.5 by default. We note that the most intense peak as well as other peaks for almost all forms of CH_2CN in the gas phase are shifted in the ice phase (Table B1). Isotopic effects on the spectral shifts is caused by differences in vibrational modes (harmonic) due to different isotopic masses. In our chemical model, we have consider two types of isotopomer of CH_2CN , namely, CHDCN and CD_2CN . They have different infrared spectra because the substitution of isotope changes the reduced mass of the corresponding molecule. In this case also, we find that the most intense mode as well as the other modes of CHDCN and CD_2CN in the gas phase are shifted in the ice phase. Infrared peak positions of CHDCN and CD_2CN with their absorbance in the gas phase as well as in other astrophysical environments are shown in Table B1. High value of the absorbance in Table B1 implies most probable transitions. According to Person & Kubulat (1990), one of the most challenging problems in the study of infrared spectroscopy is to understand the intensity of absorption by the different fundamental modes of vibration in the infrared spectrum of a molecule. Magnitudes of the integrated molar absorption coefficients are calculated by the following relation;

$$A = \frac{1}{100Cl} \int \ln(I_0/I) d\nu. \quad (1)$$

Depending on the mode of vibration and the molecule involved, the value of the absorption coefficients could vary from $0 - 10^4$ km/mol. Here, C is the concentration in mol^{-1} , l is the path length in cm, I_0 is the intensity of the light incident, I is the intensity of light transmitted and ν is the wavenumber in cm^{-1} . The factor of 100 converts the values to km/mol, with the resulting convenient range of possible values. The integration is taken over the entire absorption band. From our relative energy calculation, it is clear that the singlet state of CH_2CN^- , CHDCN^- and CD_2CN^- is the most stable spin state. From Table B1 it is evident that in case of gas phase CH_2CN^- (singlet), transition at 2056.73 cm^{-1} is the strongest one. In the ice phase, strongest transition for CH_2CN^- (singlet) comes out to be at 2016.35 cm^{-1} . Transitions at 2053.96 cm^{-1} and 2013.34 cm^{-1} are the most probable for CHDCN^- (singlet) in the gas phase and ice phase respectively. In case of CD_2CN^- (singlet), transition at 2050.23 cm^{-1} and 2009.48 cm^{-1} are the most probable in gas phase and ice phase respectively. In order to have some idea about the accuracy of our computed harmonic vibrational frequencies, we compare our result for the singlet state of CH_2CN^- with that of the Fortenberry, Crawford & Lee (2013) in Table B1. Our results appear to be reasonable.

In Fig. 1, we have shown how the isotopic substitution (CD_2CN) as well as spin multiplicity plays a part in the vibrational (harmonic) progressions of CH_2CN in the gas (denoted by G in Fig. 1), ice (denoted by I in Fig. 1). ‘Y axis’ of Fig. 1 represent the absorbance (in km/mol) and ‘X axis’ represent the wavenumber in (cm^{-1}).

3.2.2. Rotational spectroscopy

In Table 2, we have summarized our calculated rotational and distortional constants along with other spectroscopic constants for only stable spin state of CH_2CN^- , CHDCN^- and CD_2CN^- . To

have an estimation about the accuracy of our model, we compare our results with those from other existing theoretical and experimental work. Fortenberry, Crawford & Lee (2013) reported theoretically computed rotational and distortional constants along with other spectroscopic constants of CH_2CN^- using CCSD(T)/aug-cc-pVQZ level of theory. For the computation of anharmonic frequencies, analytic second derivative of energies at displaced geometries are required. But the CCSD(T) method in the Gaussian 09W program only implements energies, so analytic second derivative of energies are not available at this level of theory. So it is not possible to compute the rotational and distortional constants at CCSD(T)/aug-cc-pVQZ level of theory as used by Fortenberry, Crawford & Lee (2013) using the Gaussian 09W program. In our calculation, we have computed the rotational and distortional constants at MP2/aug-cc-pVTZ level of theory. In Table 2, we have also compared our results with the experimental results of Lykke et al. (1987) who carried out auto-detachment spectroscopy technique to study the dynamics of CH_2CN^- and one of its deuterated isotopomer (CD_2CN^-). They also reported the rotational and distortional constants of CH_2CN^- and CD_2CN^- . From Table 2, it is clear that our results are in close agreement with the theoretical and experimental work. This leads us to believe that our computed parameters for the deuterated isotopomers of CH_2CN^- could be useful for the further astronomical investigation of these molecules.

In order to summarize the results of our computation on rotational spectroscopy, we prepare our spectral information for CH_2CN^- , CHDCN^- , CD_2CN^- . In Tables B2, B3 & B4, the computed rotational transitions for the gas phase CH_2CN^- , CHDCN^- and CD_2CN^- are respectively shown. Tables B2 and B4 contain the data for CH_2CN^- and CD_2CN^- respectively. These Tables are prepared with the experimental constants (Lykke et al. 1987) given in Table 2. Here, errors on the computed line frequencies are related to the errors on the constants given in Table 2. Lykke et al., (1987) reported the rotational and distortional constants for CH_2CN^- and CD_2CN^- by fitting the observed experimental transitions with the Watson S-reduced Hamiltonian using a least square routine. Our reported spectroscopic constants are in symmetrically reduced Hamiltonian and they can be computed in Gaussian 09W program by considering anharmonic vibration-rotation coupling via perturbation theory. By following Lykke et al., (1987), in Table 2, we also have tabulated the values of 1σ in the unit of MHz in the parentheses of the corresponding experimental constants. The quantity σ corresponds to the standard deviation of the fit to the entire band. Armed with these values, we have prepared Table B2 and B4 to report the rotational transitions of CH_2CN^- and CD_2CN^- respectively. Expected errors on any line frequencies are clearly mentioned in the captions of Table B2 and B4. In case of Table B2, for the line frequencies $19\text{GHz} - 319\text{GHz}$, there could be errors in between $\pm 1 - 20\text{MHz}$ ($d\nu/\nu = 6.16 \times 10^{-5}$ for any line frequency). Similarly for Table B4, for the transitions in between $18\text{GHz} - 314\text{GHz}$, there could be errors in between $\pm 0.6 - 12\text{MHz}$ ($d\nu/\nu = 3.77 \times 10^{-5}$). Since, till now, there are no experimental constants reported for the CHDCN^- , in Table B3, we have given the information regarding the rotational transitions for CHDCN^- by using our calculated rotational and distortional constants (Table 2). Table B2, B3 and B4 are prepared by selecting only those tran-

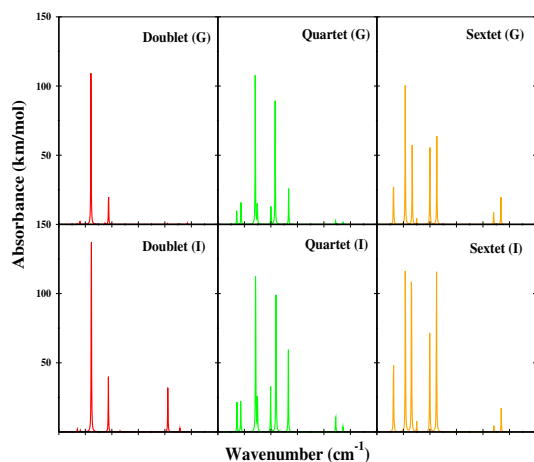


Fig. 1. Infrared spectrum of different forms of CD_2CN in gas phase, ice phase and mixed ice.

sitions which have intensities beyond $10^{-7} \text{ nm}^2 \text{ MHz}$ (base 10 logarithm of the intensities are tabulated). It is noticed that we are having several different entries of greatly differing intensities for the same line frequency. Since strongest component suffice, here (in Table B2, B3 & B4), only the component having largest intensity for the same line frequency is tabulated.

3.2.3. Electronic spectroscopy

CH_2CN^- only has one excited state (a second singlet state) in the gas phase. This has been shown experimentally (Lykke et al., 1987) and theoretically (Fortenberry & Crawford 2011a). Additionally, as for the triplet and quintet states of CH_2CN^- are above the lowest energy (doublet) state of CH_2CN radical and thus the electron will be removed from the anion before it excites into these high spin states. Hence, those states cannot exist and this is why we have not considered the higher spin states of the different forms of CH_2CN . In Fig. 2, we show the electronic absorption spectra of CH_2CN , CH_2CN^+ and CH_2CN^- for their most stable spin configuration. As per discussion in Section 3.1, doublet CH_2CN , singlet CH_2CN^+ and singlet CH_2CN^- are the most stable spin states of these species. Intense peaks in Fig. 2 are assigned due to various electronic transitions shown in Table 3. It is clear that, depending on the composition of the interstellar grain mantle, peak positions in the ice phase are shifted. Different electronic absorption spectral parameters for CH_2CN , CH_2CN^+ , CH_2CN^- in the gas phase as well as in the ice phase are given in Table 3.

4. Conclusions

There are some indications in the literature that CH_2CN^- might be the carrier of one of the many poorly characterized diffuse interstellar bands. In this paper, we investigated different ways to manifest cyanomethyl radicals in the ISM. The highlights are:

Table 2. Different spectroscopical constants of CH_2CN^- , CHDCN^- , CD_2CN^- in gas phase at MP2/aug-cc-pVTZ level of theory.

Species	Constants	Theoretical values in MHz by Fortenberry, Crawford & Lee (2013) at CCSD(T)/aug-cc-pVQZ level of theory	Experimental values in MHz (Lykke et al. (1987))	Our calculated values in MHz
CH_2CN^-	A_0	233945.4	278636.4(± 4.197095)	298584.615
	B_0	10823.22	10145.79(± 0.599585)	10069.925
	C_0	10386.01	9805.043(± 0.629564)	9687.183
	A_e	230904.9	-	287675.631
	B_e	10849.79	-	10086.765
	C_e	10445.37	-	9745.074
	τ'_{aaaa}	-100.708	-	-87.6704
	τ'_{bbbb}	-0.020	-	-0.0155
	τ'_{cccc}	-0.017	-	-0.013
	τ'_{aabb}	-1.812	-	-1.540
	τ'_{aacc}	0.043	-	-0.01594
	τ'_{bbcc}	-0.018	-	-0.01436
	D_J	0.005	0.0049465(± 0.00029979)	0.0035
	D_{JK}	0.434	0.3888308(± 0.00449689)	0.3823
	D_K	24.739	30.06319(± 0.06295642)	21.531
d_1	0.000	-0.0002698(± 0.00005396)	-0.0001297	
d_2	0.000	-0.000175678(± 0.00002308)	-0.000032387	
CHDCN^-	A_0	-	-	203788.893
	B_0	-	-	9432.261
	C_0	-	-	8960.774
	A_e	-	-	197655.384
	B_e	-	-	9454.839
	C_e	-	-	9023.214
	τ'_{aaaa}	-	-	-52.524
	τ'_{bbbb}	-	-	-0.0144
	τ'_{cccc}	-	-	-0.0115
	τ'_{aabb}	-	-	-1.268
	τ'_{aacc}	-	-	0.0469
	τ'_{bbcc}	-	-	-0.0128
	D_J	-	-	0.0031
	D_{JK}	-	-	0.2994
	D_K	-	-	12.828
d_1	-	-	-0.0001804	
d_2	-	-	-0.00005339	
CD_2CN^-	A_0	-	140757.7(± 4.496888)	147451.465
	B_0	-	9004.927(± 0.329772)	8916.168
	C_0	-	8487.186(± 0.329772)	8353.217
	A_e	-	-	143948.398
	B_e	-	-	8939.687
	C_e	-	-	8416.965
	τ'_{aaaa}	-	-	-21.951
	τ'_{bbbb}	-	-	-0.0127
	τ'_{cccc}	-	-	-0.00967
	τ'_{aabb}	-	-	-1.0326
	τ'_{aacc}	-	-	0.01407
	τ'_{bbcc}	-	-	-0.01096
	D_J	-	0.003165808(± 0.00013191)	0.0026
	D_{JK}	-	0.2320094(± 0.00233838)	0.2498
	D_K	-	7.10808(± 0.13190870)	5.235
d_1	-	-0.0000288(± 0.00004797)	-0.0001928	
d_2	-	-0.00008094(± 0.00001229)	-0.000070902	

The numbers in the parentheses represents the errors (in MHz) of the fit to the entire band obtained by Lykke et al. (1987).

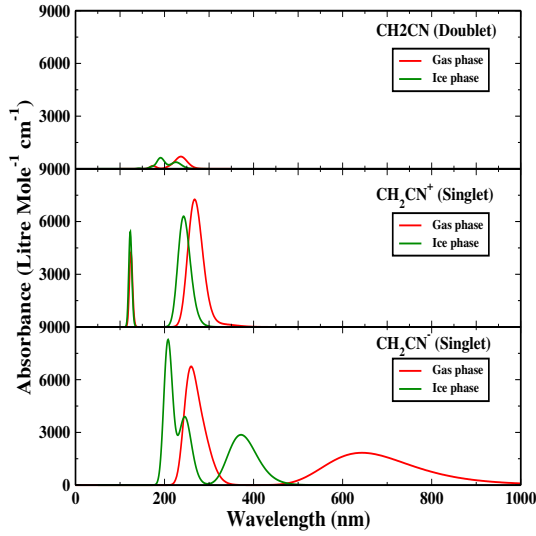


Fig. 2. Electronic absorption spectra of CH_2CN (doublet), CH_2CN^+ (singlet) and CH_2CN^- (singlet) in gas phase and in ice phase.

Table 3. Electronic transitions of the most stable spin state of CH_2CN , CH_2CN^+ and CH_2CN^- at EOM-CCSD/aug-cc-pVDZ level of theory in gas phase and water ice phase

Name & spin state	Wavelength (gas phase) (in nm)	Absorbance	Oscillator strength	Transitions	Wave length (H_2O ice) (in nm)	Absorbance	Oscillator strength	Transitions
Doublet CH_2CN	237.47	696.35	0.0167	$2-A'' \rightarrow 2-A'$	225.57	379.59	0.0093	$2-B1 \rightarrow 2-A1$
	174.07	170.09	0.0042	$2-A'' \rightarrow 2-A'$	190.29	625.57	0.0133	$2-B1 \rightarrow 2-B1$
					142.68	28.28	0.0007	$2-B1 \rightarrow 2-B2$
Singlet CH_2CN^+	267.63	7762.40	0.1793	$1-A' \rightarrow 1-A'$	242.6	6291.27	0.1538	$1-A' \rightarrow 1-A'$
	124.44	4250.86	0.1055	$1-A' \rightarrow 1-A'$	122.95	5423.60	0.1346	$1-A' \rightarrow 1-A'$
Singlet CH_2CN^-	643.5	1838.62	0.0454	$1-A' \rightarrow 1-A''$	371.74	2862.63	0.0707	$1-A' \rightarrow 1-A''$
	257.03	6743.34	0.1528	$1-A' \rightarrow 1-A'$	245.92	3892.09	0.0951	$1-A' \rightarrow 1-A'$
					207.81	8252.17	0.20411	$1-A' \rightarrow 1-A'$

- We performed quantum chemical calculations to find out energetically the most stable spin configuration for various forms of CH_2CN .
- By introducing a large deuterated network into our chemical model, we have explored the existence of different isotopologues of CH_2CN , CH_2CN^+ and CH_2CN^- (provided in the Appendix). Our chemical modeling shows that different isotopomers of various forms of CH_2CN could efficiently be formed in the ISM. Column densities of various isotopomers of cyanomethyl anions are reasonably higher and could be observed with the present instrumental facility, like, ALMA, JVLA etc..
- We explored the vibrational (harmonic), rotational and electronic spectral properties of different forms of CH_2CN in different astrophysical environments. Our result could be used as a guideline for observing various forms of CH_2CN around ISM. In the Appendix, we have pre-

sented the rotational transitions of CH_2CN^- , CHDCN^- and CD_2CN^- which could be useful for observational identifications.

Acknowledgments

LM is grateful to DST for partial financial support through a project (Grant No. SR/S2/HEP-40/2008) and AD wants to thank the ISRO respond project (Grant No. ISRO/RES/2/372/11-12). The authors would like to thank the anonymous referee and Prof. Malcolm Walmsley whose valuable suggestions have helped to improve this paper significantly.

References

- Agundez, M., Fonfria, J. P., Cernicharo, J., Pardo, J. R., & Guelin, M. 2008, *A&A*, 479, 493
- Allen, M., Robinson, G. W., 1977., *ApJ*, 212, 396
- Albertsson, T., Semenov, D. A., Vasyunin, A. I., Henning T., Herbst, E., 2013, *APJS*, 207, 27
- Arzoumanian, D., Andr , P., Didelon, P., et al. 2011, *A&A*, 529, L6+
- Becke A. D., 1993, *J. Chem. Phys.*, 98, 5648
- Chakrabarti, S., Chakrabarti, S.K., 2000a. *A&A* 354, L6
- Chakrabarti, S. K., Chakrabarti, S., 2000b. *Ind. J. Phys* 74B, 97
- Chakrabarti, S.K., Das, A., Acharyya, K., Chakrabarti, S., 2006, *A&A*, 457, 167
- Chakrabarti, S.K., Das, A., Acharyya, K., Chakrabarti, S., 2006, *BASI*, 34, 299
- Churchwell, E. 1980, *ApJ*, 240, 811
- Clouthier, D. J., Moule, D.C., 1987, *J. Am. Chem. Soc.* 109, 6259
- Cordiner, M. A., & Sarre, P. J. 2007, *A&A*, 472, 537
- Cuppen, H. M., Herbst, E., 2007, *APJ*, 668, 294
- Cuppen, H. M., Van Dishoeck E., F., Herbst, E., Tielens, A. G. G. M., 2009, *A&A*, 508, 275
- Cummins, S. E., Line, R. A., Thaddeus, P., 1986, *APJS*, 60, 819
- Das, A. Majumdar, L., Chakrabarti, S. K., & Chakrabarti S., 2013a, *New Astronomy*, 23, 118
- Das, A. Majumdar, L., Chakrabarti, S. K., Saha, R., Chakrabarti S., 2013b, *MNRAS*, 433, 3152
- Das, A., Acharyya, K., Chakrabarti, S. & Chakrabarti, S. K., 2008b, *A&A*, 486, 209
- Das, A., Acharyya, K. & Chakrabarti, S. K., 2010, *MNRAS* 409, 789
- Das, A., Chakrabarti, S. K., Acharyya K. & Chakrabarti, S., 2008a, *NEWA*, 13, 457
- Das, A. & Chakrabarti, S. K., 2011, *MNRAS*, 418, 545
- Demyk, K., Dartois, E., dHendecourt, L., Jourdain de Muizon, M., Heras, A. M., Breitfellner, M. 1998, *A&A*, 339, 553
- Fortenberry, R. C. Crawford, T. D., Lee, J., T., 2013, *ApJ*, 762, 121
- Fortenberry, R. C., Huang, X., Francisco, J. S., Crawford, T. D., Lee, T. J., 2012a, *JPCA*, 116, 9582
- Fortenberry, R. C., Huang, X., Francisco, J. S., Crawford, T. D., Lee, T. J., 2012b, *JChPh*, 136, 234309
- Fortenberry, R. C. Crawford, T. D., 2011a, *J. Chem. Phys.*, 134, 154304
- Fortenberry, R. C., Crawford, T. D., 2011b, *Annu. Rep. Comput. Chem.*, 7, 195
- Fortenberry, R. C., Crawford, T. D., 2011c, *JPCA*, 115, 8119
- Frisch, M. J.; Trucks, G. W.; Schlegel, H. B., et al. 2009, *Gaussian 09*, Revision D.01, D. J. Gaussian, Inc., Wallingford CT

- Gerin, M., Combes, F., Encrenaz, P., Turner, B., Wootten, A., Bogey, M., Destombes, J.L., 1989, *A&A*, 224, L24-L26
- Gibb, E. L., et al. 2000, *ApJ*, 536, 347
- Goldsmith, P. F., Heyer, M., Narayanan, G., et al. 2008, *ApJ*, 680, 428
- Hasegawa, T., Herbst, E., Leung, C.M., 1992, *APJ*, 82, 167
- Hasegawa, T., Herbst, E., 1993, *MNRAS*, 261, 83
- Herbig, G. H. 1995, *Annu. Rev. Astrophys.*, 33, 19
- Herbst, E. 2001, *Chem. Soc. Rev.*, 30, 168
- Herbst, E., 1985, *ApJ*, 291, 226
- Herbst, E. 2006, in *Springer Handbook of Atomic, Molecular, and Optical Physics*, ed. G. W. F. Drake (New York: Springer), 561
- Smith, I.W.M., Herbst, E., Chang, Q., 2004, *MNRAS*, 350
- Huang, X., Lee, T. J. 2008, *JChPh*, 129, 044312
- Huang, X., Lee, T. J. 2009, *JChPh*, 131, 104301
- Huang, X., Lee, T. J. 2011, *ApJ*, 736, 33
- Hudson, R. L., Moore, M. H., Gerakines, P. A. 2001, *ApJ*, 550, 1140
- Inostroza, N., Huang, X., Lee, T. J. 2011, *JChPh*, 135, 244310
- Irvine, W. M., Friberg, P., Hjalmarsen, A., et al. 1988, *ApJ*, 334, L107
- Lee, H., H., Herbst, E., Pineau des Forets, G., Roueff, E., Le Bourlot, J., 1996, *A&A*, 311, 690
- Lee C., Yang W., Parr R. G., 1988, *Phys. Rev. B*, 58, 785
- Leitch-Devlin, M., A., Williams, D., A., 213, 295, *MNRAS*, 1985
- Linsky, J.L., Diplas, A., Wood, B.E., Brown, A., Ayres, T.R., Savage, B.D., 1995. *ApJ*. 451, 335B351
- Lykke K. R., Neumark D. M., Andersen T., Trapa V. J., Lineberger W. C., 1987, *J. Chem. Phys.*, 87, 6842
- Person, W. B., Kubulat, K., *J. Mol. Struc.*, 1990, 224, 225
- Majumdar, L., Das, A., Chakrabarti, S.K., Chakrabarti, S., 2013, *New Astronomy*, 20, 15
- Majumdar, L., Das, A., Chakrabarti, S.K., Chakrabarti, S., 2012, *Research in Astronomy & Astrophysics*, 12, 1613
- McElroy, D., Walsh, C., Markwick, A. J., Cordiner, M. A., Smith, K., Millar, T. J., 2013 *A&A*, 550, A36
- Novozamsky, J. H., Schutte, W. A., Keane, J. V. 2001, *A&A*, 379, 588
- Nutter, D., Kirk, J. M., Stamatellos, D., Ward-Thompson, D. 2008, *MNRAS*, 384, 755
- Ohishi M., Irvine, W. M., Kaifu, N., 1992, *IAUS*, 150, 1710
- Ostriker, J. 1964, *ApJ*, 140, 1056
- Ozeki, H., Hirao, T., Saito, S., & Yamamoto, S. 2004, *ApJ*, 617, 680
- Park, J. Y. & Woon, D. E., 2006, *APJ*, 648, 1285
- Palmeirim, P., Ph. Andre, Ph., Kirk, J. et al. 2013, *A&A*, 550, 38
- Pascual-Ahuir, J. L., Silla, E., Tun, I., *J. Comp. Chem.*, 1994, 15, 1127
- Pickett, H. M., *J. Mol. Spectrosc.*, 1991, 148, 371
- Pilbratt, G. L., Riedinger, J. R., Passvogel, T., et al. 2010, *A&A*, 518, L1+
- Roberts, H., Millar, T. J., 2000, *A&A*, 361, 388
- Prasad, S. S., Huntress Jr., W. T, 1980, *APJS*, 43, 1
- Sarre, P. J. 2006, *J. Mol. Spec.*, 238, 1
- Sarre, P. J. 2000, *MNRAS*, 313, L14

- Schutte, W. A., & Greenberg, J. M. 1997, A&A, 317, L43
- Schutte, W. A., Greenberg, J. M., van Dishoeck, E. F., Tielens, A. G. G. M., Boogert, A. C. A., Whittet, D. C. B. 1997, Ap&SS, 255, 61
- Schutte, W. A., et al. 1999, A&A, 343, 966
- Shalabiea, O. M., greenberg, J. M., 1994, A&A, 290, 266
- Stantcheva, T., Shematovich, V. I., Herbst, E., 2002, A&A, 391, 1069
- Soifer, B. T., Puetter, R. C., Russell, R. W., Willner, S. P., Harvey, P. M., Gillett, F. C. 1979, ApJ, 232, L53
- Schneider, S., Elmegreen, B. G. 1979, ApJS, 41, 87
- Su, T., & Chesnavich, W. J. 1982, J. Chem. Phys., 76, 5183
- Tielens A. G. G. M., Tokunaga A. T., Geballe T. R., Baas F., 1991, ApJ, 381, 181
- Tomasi, J., Cammi, R., Mennucci, B., Cappelli, C., and Corni, S., Phys. Chem. Chem. Phys., 2002, 4, 5697
- Tomasi, J., Mennucci, B., Cammi, R., Chem. Rev., 2005, 105, 2999
- Tomasi, J., Mennucci, B., Cancs, E., J. Mol. Struct. (Theochem), 1999, 464, 211
- Turner, B. E., 2001, APJS, 136, 579
- Woon, D. E., Herbst, E., 2009, APJS, 185, 273
- Woodall, J., Agnèz, M., Markwick-Kemper, A.J., Millar, T.J., 2007, A&A, 466, 1197

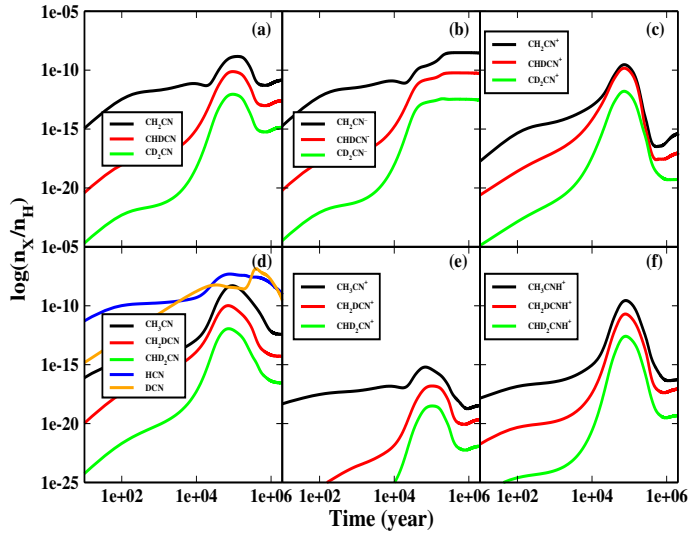


Fig. A1. (a-f). Chemical evolution of the cyanomethyl radical and its related species.

Appendix A

Chemical modeling:

In order to study various forms of the cyanomethyl radical in the interstellar medium (ISM), we develop a chemical model which includes the gas phase as well as the grain surface chemical network. Our gas phase chemical network consists of the network of Woodall et al. (2007) and the deuterated network used in Das et al. (2013b). Moreover, we include certain new reactions for the formation and destruction of various forms of cyanomethyl radical and its related species. Our surface network mainly adopted from Das et al. (2013b) and references therein. Our present gas phase chemical network consists of 6296 reactions and present surface chemical network consists of 285 reactions. Except molecular hydrogen (according to Leitch & Williams 1985, sticking coefficient of $H_2 \sim 0$) and Helium (Roberts & Millar 2000 assumed that Helium would not stick to the grain), depletion of all the gas phase neutral species onto the grain surface are considered with a sticking probability one.

In Table A1, we have presented only those reactions which are responsible for the formation and destruction of various deuterated isotopomers of cyanomethyl radical and its related species. Various types of reactions are considered in the network, namely, ion(cation)-neutral (IN), neutral-neutral (NN), charge exchange (CE), dissociative recombination (DR), photo-dissociation (PH), cosmic ray induced photo-dissociation (CRP), radiative association (RA), associative detachment (AD), radiative electron attachment (REA) and mutual neutralization (MN). The reaction network given in Table A1 is constructed mainly by assuming that reaction pathways are similar as those of hydrogenated reactions in Woodall et al. (2007). Following are

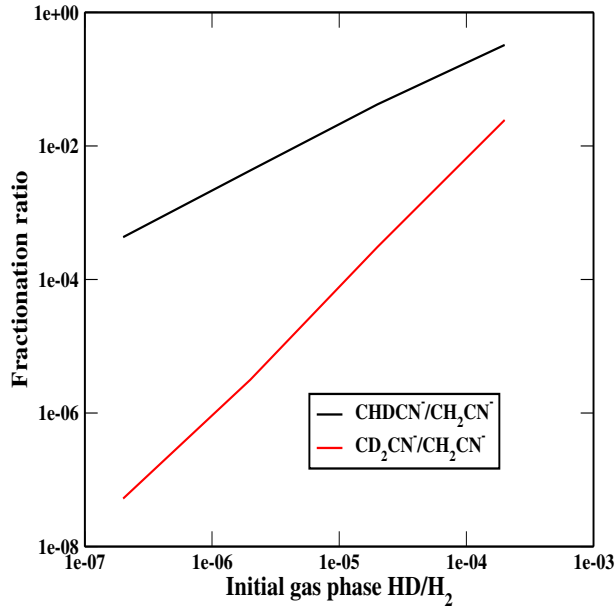


Fig. A2. Variation of fractionation ratio of CH_2CN^- with the initial gas phase fractionation ratio (abundance of HD/abundance of H_2).

the adequate discussion regarding the adopted network for the various forms of cyanomethyl radical and its related species.

Ion-neutral:

Ion(cation)-neutral reactions ($A^+ + B \rightarrow C^+ + D$) are the dominant means for the destruction of a neutral interstellar species. All the deuterated ion neutral reactions are assumed to be similar to the corresponding hydrogenated reactions given in the network of Woodall et al. (2007). The reaction numbers from R1 to R55 of Table A1 are of this kind. According to Herbst (2006), for a ion-molecular reaction, rate coefficient can be determined using the capture theory where the translational energy of the reactant must only surpass a lon-range centrifugal barrier for the reaction to occur. The collision rate coefficient between an ion and non-polar neutral molecule can be determined using the so called Langevin collision rate

$$k_L = 2\pi e \sqrt{\frac{\alpha_d}{\mu}}, \quad (2)$$

where, e is the electronic charge, α is the polarizability of the neutral non-polar molecule in Å^3 , μ is the reduced mass of the reactants. But for polar neutral species, a complex situation arises due to the attraction between a charge and rotating permanent dipole moment. Su & Chesnavich, (1982) predicted the rate coefficients for this type of reactions. According to Woon & Herbst, (2009), the Su-Chesnavich formula can be written in two different ways and both of which uses

a parameter

$$x = \mu_D / \sqrt{2\alpha kT},$$

where k is the Boltzmann constant, μ_D is the dipole moment of the polar neutral species in Debye & T is the temperature in Kelvin. Depending on the values of 'x', rate coefficients could be calculated by following two equations;

$$k_{IN} = (0.4767x + 0.6200) k_L \text{ for } x \geq 2, \quad (3)$$

$$k_{IN} = [(x + 0.5090)^2 / 10.526 + 0.9754] k_L \text{ for } x < 2. \quad (4)$$

Note that for $x = 0$, above equations reduces to the Langevin expression. Alternatively, Woon & Herbst (2009) expressed the equation for $x \geq 2$ in powers of temperature T as following;

$$k_{IN} = c_1 + c_2 / \sqrt{T}, \quad (5)$$

where, $c_1 = 0.62 k_L$ and $c_2 = (0.4767\mu_D / \sqrt{2\alpha k}) k_L$.

For the computation of the rate coefficients, value of the polarizability and the dipole moment of the neutral molecules are taken from Woon & Herbst (2009). Here we have considered that polarizability and dipole moment will be invariant under the isotopic substitution. Theoretical computation of the polarizability and dipole moment depends on the derivatives of the electronic energy with respect to the external electric field. Since this electronic energy is not dependent on the mass of the nuclei (as the calculations are based on the Born-Oppenheimer approximation), isotopic substitution will not affect the results. But, since isotopic substitution changes the effective reduced mass of the reactants, the rate coefficients for the deuterated reactions could be different. Computed rate coefficients for the reaction numbers from R1 to R55 are also given in Table A1 for $T = 10K$. Polarizability of the neutral reactants in the unit of Å^3 and their respective dipole moments in the unit of Debye which are used for the computation of the rate coefficients are also given in Table A1.

Neutral-neutral:

Reaction numbers R56 to R58 of Table A1 are the neutral-neutral ($A+B \rightarrow C+D$) type reactions. From Woodall et al. (2007), we took those neutral-neutral reactions where neutral CH_2CN is involved and assumed that similar reactions would be possible for its deuterated isotopomers. For the computation of rate coefficients for the neutral-neutral reactions, one needs to calculate the electronic energy barrier. But this electronic energy barrier is independent of the atomic mass. Due to this reason, we have assumed that the rate coefficients would be similar to those values for neutral CH_2CN in Woodall et al. (2007). In Woodall et al. (2007), rate coefficients of this type of reactions were calculated by;

$$k_{NN} = \alpha \left(\frac{T}{300}\right)^\beta \exp\left(\frac{-\gamma}{T}\right), \quad (6)$$

where, α, β and γ are the three constants. For reaction R56 & R57, we have assumed that $\alpha = 1 \times 10^{-10}$, $\beta = 0$ and $\gamma = 0$ by following the reaction $C + CH_2CN \rightarrow HC_3N + H$ in Woodall et al. (2007) (Smith, Herbst & Chang 2004) and for the reaction R58, we have assumed $\alpha = 6.2 \times 10^{-11}$, $\beta = 0$ and $\gamma = 0$ by following the reaction $N + C_2H_3 \rightarrow CH_2CN + H$ in Woodall et al. (2007). Woodall et al., (2007), used these rate coefficients by following Smith, Herbst & Chang (2004).

Charge Exchange:

Charge Exchange ($A^+ + B \rightarrow A + B^+$) type reactions are very common in the ISM. We have considered eight reactions (R59-R66) which are of this type. Rate constants (α, β & γ) of these reactions are also assumed to be similar to their hydrogenated counterpart as mentioned in Woodall et al. (2007) and the rate coefficients are calculated by using Eqn. 6. Woodall et al. (2007) used $\alpha = 6.3 \times 10^{-9}$, $\beta = 0$ and $\gamma = 0$ for $H^+ + CH_2CN \rightarrow CH_2CN^+ + H$. We have assumed that these values are also applicable for the reactions containing deuterated isotopomers of CH_2CN .

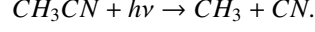
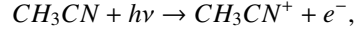
Dissociative Recombination:

Interstellar cations are mainly destroyed by the dissociative recombination ($A + e^- \rightarrow C + D$) processes. In our network, R67-R78 are of this kind. Dissociative recombination reaction pathways for the deuterated species are developed by following the pathways available for CH_3CN^+ , CH_3CNH^+ , CH_2CN^+ from Woodall et al. (2007). Rate coefficients for the reaction numbers from R67 to R78 are computed by using eqn. 2. As before, here also, we have assumed that the isotopic substitution does not influence the computed rate coefficients very much. The rate constants (α, β & γ) of the deuterated reactants are assumed to be similar to the hydrogenated reactions in Woodall et al. (2007). For the reaction R67-R78, $\alpha = 1.5 \times 10^{-7}$, $\beta = -0.5$ and $\gamma = 0$ are used by following the DR channel of CH_3CN^+ , CH_3CNH^+ , CH_2CN^+ used in Woodall et al. (2007). Typical values of these kind of rate coefficients are of the order of $\sim 10^{-7} \text{ cm}^3 \text{ s}^{-1}$.

Photo-dissociation:

Reaction numbers R79 to R82 of Table A1 are the photo-dissociation type reactions ($AB + h\nu \rightarrow A + B/AB + h\nu \rightarrow AB^+ + e^-$). These reactions are taken from Woodall et al. (2007) and are applied for the deuterated reactions as well. They have considered these dissociation reactions for CH_3CN and here, we assumed that these dissociation reactions are also possible for CH_2DCN and CHD_2CN . For the photo-dissociation reaction of CH_3CN , Woodall et al. (2007) assumed that

there would be two branching ratio;



For the first reaction, $\alpha = 6.2 \times 10^{-10}$, $\beta = 0$ and $\gamma = 3.1$ were assumed and for the second reaction, $\alpha = 3.4 \times 10^{-9}$, $\beta = 0$ and $\gamma = 2.0$ were assumed. Here, we have adopted similar values for the deuterated reactions. Following Woodall et al. (2007), the rate coefficient for these reactions could be adopted as following:

$$k_{pH} = \alpha \exp(\gamma A_V) s^{-1}, \quad (7)$$

where, A_V is the visual extinction parameter. In Table A1, we presented the rate coefficients for all the reactions having $T=10K$ and $A_V=10$ (cold and dense cloud condition).

Cosmic ray induced photo-dissociation:

In Table A1, the reaction numbers from R83 to R86 are for cosmic ray induced photo dissociation ($A + CRP \rightarrow A^+ + e^- / A + CRP \rightarrow C + D$). Rate coefficients for these kind of reactions could be adopted as follows:

$$k_{CR}(T) = \alpha \left(\frac{T}{300}\right)^\beta \frac{\gamma}{(1 - \omega)}, \quad (8)$$

where, α is the cosmic-ray ionization rate, γ is the probability per cosmic-ray ionization that the appropriate photo reaction taking place, and ω is the dust grain albedo in the far ultraviolet. Following Woodall et al. (2007), we use the cosmic ray ionization rate of $\alpha = 1.3 \times 10^{-17}$ and $\omega=0.6$. These reactions (R83-R86) are taken from Woodall et al. (2007) and are applied for the deuterated reactions here. Woodall et al. (2007) assumed two photo-dissociation channel for CH_3CN . They used $\gamma = 1122.5$ & 2388.0 and $\beta = 0$ & 0 for these two channels respectively. We have used same values of β & γ for the dissociation channels of CH_2DCN and CHD_2CN .

Radiative association:

The reaction numbers from R87 to R90 of Table A1 are the radiative association type reactions ($A + B \rightarrow C + h\nu$). These reactions along with the rate coefficients are taken from the hydrogenated reactions of Woodall et al. (2007) and applied here for the deuterated reactions. Rate coefficients of these reactions are calculated by using Eqn. 6. Following the reaction $CH_3 + CN \rightarrow CH_3CN + h\nu$ in Woodall et al. (2007), we have assumed that reaction R87 and R89 would also possible with $\alpha = 1 \times 10^{-16}$, $\beta = 0$ and $\gamma = 0$. Woodall et. al., (2007) considered this rate coefficients by following Prasad & Huntress (1980). Similarly, by following the reaction $CH_3^+ + HCN \rightarrow CH_3CNH^+ + h\nu$ in Woodall et al. (2007) (they adopted it from Herbst 1985), we have assumed that similar reaction would be possible for the deuterated species (reaction

R88 and R90) having $\alpha = 9.0 \times 10^{-9}$, $\beta = -0.5$ and $\gamma = 0$.

Associative detachment:

R91 & R92 of Table A1 are the associative detachment type ($A + B^- \rightarrow C + e^-$) reactions. These are taken from Woodall et al. (2007) for the formation of CH_3CN and are applied here for the deuterated reactions. Rate constants are assumed to be the same and are computed by using Eqn. 6. $\alpha = 1 \times 10^{-9}$, $\beta = 0$ and $\gamma = 0$, were adopted in Woodall et al. (2007) for the reaction $\text{CH}_3 + \text{CN}^- \rightarrow \text{CH}_3\text{CN} + e^-$, here we assumed similar values of α , β and γ for the reaction R91 and R92.

Radiative electron attachment:

The anions (CH_2CN^- , CHDCN^- & CD_2CN^-) are formed primarily via radiative electron attachment ($A + e^- \rightarrow A^- + h\nu$) reactions (the reaction numbers from R93 to R95 of Table A1). Following McElroy et al. (2009), we have adopted the following formula for the computation of the rate coefficient of this type:

$$k_{\text{REA}} = 1.25 \times 10^{-7} \left(\frac{T}{300}\right)^{-0.5} \text{ cm}^3 \text{ s}^{-1}. \quad (9)$$

Mutual neutralization:

Interstellar anions could efficiently be destroyed by the cations. These type of reactions are called mutual neutralization reaction ($A^- + B^+ \rightarrow A + B$). Reaction number R96 to R116 of Table A1 are of this type. According to Das et al. (2013b), H_3^+ , C^+ , H_3O^+ , HCO^+ , HN_2^+ , O^+ and H^+ are the major interstellar cations. For the mutual neutralization reactions, we have taken the reactions between these cations and different isotopomers of CH_2CN^- . Following Walsh et al. (2009), the rate coefficients of these reactions are computed by following relationship:

$$k_{\text{MN}} = 7.5 \times 10^{-8} \left(\frac{T}{300}\right)^{-0.5} \text{ cm}^3 \text{ s}^{-1}. \quad (10)$$

Table A1. Added Reaction network for cyanomethyl radical and its related species.

Reaction number	Reaction type	Reaction pathways for different isotopomers of Cyanomethyl radical	Rate coefficient at T=10K $A_V = 10$
R1	IN	$H_3^+ + CD_2CN (4.382, 3.499^a) \rightarrow CH_2DCN^+ + HD$	$4.60 \times 10^{-08} \text{ cm}^3 \text{ s}^{-1}$
R2	IN	$He^+ + CD_2CN (4.382, 3.499^a) \rightarrow CN + CD_2^+ + He$	$5.58 \times 10^{-08} \text{ cm}^3 \text{ s}^{-1}$
R3	IN	$CHD_2CN^+ + CO (1.951, 0.101^a) \rightarrow CD_2CN + HCO^+$	$1.04 \times 10^{-09} \text{ cm}^3 \text{ s}^{-1}$
R4	IN	$H^+ + CHD_2CN (4.315, 3.932^a) \rightarrow CD_2CN^+ + H_2$	$8.72 \times 10^{-08} \text{ cm}^3 \text{ s}^{-1}$
R5	IN	$CD_2^+ + HCN (2.497, 3.007^a) \rightarrow CD_2CN^+ + H$	$2.08 \times 10^{-08} \text{ cm}^3 \text{ s}^{-1}$
R6	IN	$C_2HD^+ + ND (1.447, 1.522^a) \rightarrow CD_2CN^+ + H$	$1.07 \times 10^{-08} \text{ cm}^3 \text{ s}^{-1}$
R7	IN	$CHD_2^+ + CN (2.884, 1.390^a) \rightarrow CD_2CN^+ + H$	$9.94 \times 10^{-09} \text{ cm}^3 \text{ s}^{-1}$
R8	IN	$C_2D^+ + NHD (1.782, 1.768^a) \rightarrow CD_2CN^+ + H$	$1.22 \times 10^{-08} \text{ cm}^3 \text{ s}^{-1}$
R9	IN	$C_2D^+ + NH_2D (2.087, 1.519^a) \rightarrow CD_2CN^+ + H_2$	$1.05 \times 10^{-08} \text{ cm}^3 \text{ s}^{-1}$
R10	IN	$H^+ + CH_2DCN (4.315, 3.932^a) \rightarrow CHDCN^+ + H_2$	$8.72 \times 10^{-08} \text{ cm}^3 \text{ s}^{-1}$
R11	IN	$H^+ + CH_2DCN (4.315, 3.932^a) \rightarrow CH_2D^+ + HCN$	$8.72 \times 10^{-08} \text{ cm}^3 \text{ s}^{-1}$
R12	IN	$H^3 + +CH_2DCN (4.315, 3.932^a) \rightarrow CH_2DCNH^+ + H_2$	$5.15 \times 10^{-08} \text{ cm}^3 \text{ s}^{-1}$
R13	IN	$He^+ + CH_2DCN (4.315, 3.932^a) \rightarrow CN + CH_2D^+ + He$	$6.24 \times 10^{-08} \text{ cm}^3 \text{ s}^{-1}$
R14	IN	$H_3O^+ + CH_2DCN (4.315, 3.932^a) \rightarrow CH_2DCNH^+ + H_2O$	$2.38 \times 10^{-08} \text{ cm}^3 \text{ s}^{-1}$
R15	IN	$C_2H_2^+ + CH_2DCN (4.315, 3.932^a) \rightarrow CH_2DCNH^+ + C_2H$	$2.15 \times 10^{-08} \text{ cm}^3 \text{ s}^{-1}$
R16	IN	$HCNH^+ + CH_2DCN (4.315, 3.932^a) \rightarrow CH_2DCNH^+ + HCN$	$2.10 \times 10^{-08} \text{ cm}^3 \text{ s}^{-1}$
R17	IN	$HCNH^+ + CH_2DCN (4.315, 3.932^a) \rightarrow CH_2DCNH^+ + HNC$	$2.10 \times 10^{-08} \text{ cm}^3 \text{ s}^{-1}$
R18	IN	$HCO^+ + CH_2DCN (4.315, 3.932^a) \rightarrow CH_2DCNH^+ + CO$	$2.08 \times 10^{-08} \text{ cm}^3 \text{ s}^{-1}$
R19	IN	$HN_2^+ + CH_2DCN (4.315, 3.932^a) \rightarrow CH_2DCNH^+ + N_2$	$2.08 \times 10^{-08} \text{ cm}^3 \text{ s}^{-1}$
R20	IN	$C_2H_5^+ + CH_2DCN (4.315, 3.932^a) \rightarrow CH_2DCNH^+ + C_2H_4$	$2.08 \times 10^{-08} \text{ cm}^3 \text{ s}^{-1}$
R21	IN	$HCO_2^+ + CH_2DCN (4.315, 3.932^a) \rightarrow CO_2 + CH_2DCNH^+$	$1.85 \times 10^{-08} \text{ cm}^3 \text{ s}^{-1}$
R22	IN	$HCOOH_2^+ + CH_2DCN (4.315, 3.932^a) \rightarrow CH_2DCNH^+ + HCOOH$	$1.83 \times 10^{-08} \text{ cm}^3 \text{ s}^{-1}$
R23	IN	$HC_3NH^+ + CH_2DCN (4.315, 3.932^a) \rightarrow CH_2DCNH^+ + HC_3N$	$1.79 \times 10^{-08} \text{ cm}^3 \text{ s}^{-1}$
R24	IN	$H_3^+ + CHDCN (4.382, 3.499^a) \rightarrow CH_2DCN^+ + H_2$	$4.61 \times 10^{-08} \text{ cm}^3 \text{ s}^{-1}$
R25	IN	$C_2HD^+ + NH_2 (1.782, 1.768^a) \rightarrow CH_2DCN^+ + H$	$1.24 \times 10^{-08} \text{ cm}^3 \text{ s}^{-1}$
R26	IN	$CH_2DCN^+ + CO (1.951, 0.101^a) \rightarrow CHDCN + HCO^+$	$1.04 \times 10^{-09} \text{ cm}^3 \text{ s}^{-1}$
R27	IN	$CH_2DCN^+ + H_2 (0.773, 0^a) \rightarrow CH_2DCNH^+ + H$	$1.48 \times 10^{-09} \text{ cm}^3 \text{ s}^{-1}$
R28	IN	$C_2H_7^+ + DCN (2.497, 3.007^a) \rightarrow CH_2DCNH^+ + CH_4$	$1.71 \times 10^{-08} \text{ cm}^3 \text{ s}^{-1}$
R29	IN	$CH_3OH_2^+ + DCN (2.497, 3.007^a) \rightarrow CH_2DCNH^+ + H_2O$	$1.69 \times 10^{-08} \text{ cm}^3 \text{ s}^{-1}$
R30	IN	$HCOOH_2^+ + CH_2DCN (4.315, 3.932^a) \rightarrow CH_2DCNH^+ + HCOOH$	$1.83 \times 10^{-08} \text{ cm}^3 \text{ s}^{-1}$
R31	IN	$HC_3NH^+ + CH_2DCN (4.315, 3.932^a) \rightarrow CH_2DCNH^+ + HC_3N$	$1.78 \times 10^{-08} \text{ cm}^3 \text{ s}^{-1}$
R32	IN	$H^+ + CHD_2CN (4.315, 3.932^a) \rightarrow CHD_2^+ + HCN$	$8.72 \times 10^{-08} \text{ cm}^3 \text{ s}^{-1}$
R33	IN	$H^3 + +CHD_2CN (4.315, 3.932^a) \rightarrow CHD_2CNH^+ + H_2$	$5.14 \times 10^{-08} \text{ cm}^3 \text{ s}^{-1}$
R34	IN	$He^+ + CHD_2CN (4.315, 3.932^a) \rightarrow CN + CHD_2^+ + He$	$6.23 \times 10^{-08} \text{ cm}^3 \text{ s}^{-1}$
R35	IN	$H_3O^+ + CHD_2CN (4.315, 3.932^a) \rightarrow CHD_2CNH^+ + H_2O$	$2.37 \times 10^{-08} \text{ cm}^3 \text{ s}^{-1}$
R36	IN	$C_2H_2^+ + CHD_2CN (4.315, 3.932^a) \rightarrow CHD_2CNH^+ + C_2H$	$2.14 \times 10^{-08} \text{ cm}^3 \text{ s}^{-1}$
R37	IN	$HCNH^+ + CHD_2CN (4.315, 3.932^a) \rightarrow CHD_2CNH^+ + HCN$	$2.09 \times 10^{-08} \text{ cm}^3 \text{ s}^{-1}$
R38	IN	$HCNH^+ + CHD_2CN (4.315, 3.932^a) \rightarrow CHD_2CNH^+ + HNC$	$2.09 \times 10^{-08} \text{ cm}^3 \text{ s}^{-1}$
R39	IN	$HCO^+ + CHD_2CN (4.315, 3.932^a) \rightarrow CHD_2CNH^+ + CO$	$2.07 \times 10^{-08} \text{ cm}^3 \text{ s}^{-1}$
R40	IN	$HN_2^+ + CHD_2CN (4.315, 3.932^a) \rightarrow CHD_2CNH^+ + N_2$	$2.07 \times 10^{-08} \text{ cm}^3 \text{ s}^{-1}$
R41	IN	$C_2H_5^+ + CHD_2CN (4.315, 3.932^a) \rightarrow CHD_2CNH^+ + C_2H_4$	$2.07 \times 10^{-08} \text{ cm}^3 \text{ s}^{-1}$
R42	IN	$HCO_2^+ + CHD_2CN (4.315, 3.932^a) \rightarrow CO_2 + CHD_2CNH^+$	$1.83 \times 10^{-08} \text{ cm}^3 \text{ s}^{-1}$
R43	IN	$HCOOH_2^+ + CHD_2CN (4.315, 3.932^a) \rightarrow CHD_2CNH^+ + HCOOH$	$1.81 \times 10^{-08} \text{ cm}^3 \text{ s}^{-1}$
R44	IN	$HC_3NH^+ + CHD_2CN (4.315, 3.932^a) \rightarrow CHD_2CNH^+ + HC_3N$	$1.78 \times 10^{-08} \text{ cm}^3 \text{ s}^{-1}$
R45	IN	$H_3^+ + CD_2CN (4.382, 3.499^a) \rightarrow CHD_2CN^+ + H_2$	$4.60 \times 10^{-08} \text{ cm}^3 \text{ s}^{-1}$
R46	IN	$C_2HD^+ + NHD (1.782, 1.768^a) \rightarrow CHD_2CN^+ + H$	$1.21 \times 10^{-08} \text{ cm}^3 \text{ s}^{-1}$
R47	IN	$CHD_2CN^+ + H_2 (0.773, 0^a) \rightarrow CHD_2CNH^+ + H$	$1.48 \times 10^{-09} \text{ cm}^3 \text{ s}^{-1}$
R48	IN	$H_3^+ + CHD_2CN (4.315, 3.932^a) \rightarrow CHD_2CNH^+ + H_2$	$5.14 \times 10^{-08} \text{ cm}^3 \text{ s}^{-1}$
R49	IN	$CH_3OHD^+ + DCN (2.497, 3.007^a) \rightarrow CHD_2CNH^+ + H_2O$	$1.68 \times 10^{-08} \text{ cm}^3 \text{ s}^{-1}$
R50	IN	$He^+ + CHDCN (4.382, 3.499^a) \rightarrow CN + CHD^+ + He$	$5.58 \times 10^{-08} \text{ cm}^3 \text{ s}^{-1}$
R51	IN	$CHD^+ + HCN (2.497, 3.007^a) \rightarrow CHDCN^+ + H$	$2.12 \times 10^{-08} \text{ cm}^3 \text{ s}^{-1}$
R52	IN	$C_2HD^+ + NH (1.447, 1.522^a) \rightarrow CHDCN^+ + H$	$1.09 \times 10^{-08} \text{ cm}^3 \text{ s}^{-1}$
R53	IN	$CH_2D^+ + CN (2.884, 1.390^a) \rightarrow CHDCN^+ + H$	$1.01 \times 10^{-08} \text{ cm}^3 \text{ s}^{-1}$
R54	IN	$C_2D^+ + NH_2 (1.782, 1.768^a) \rightarrow CHDCN^+ + H$	$1.25 \times 10^{-08} \text{ cm}^3 \text{ s}^{-1}$
R55	IN	$C_2D^+ + NH_3 (2.087, 1.519^a) \rightarrow CHDCN^+ + H_2$	$1.06 \times 10^{-08} \text{ cm}^3 \text{ s}^{-1}$

Reaction number	Reaction type	Reaction pathways for different isotopomers of Cyanomethyl radical	Rate coefficient at $T=10K$ $A_V = 10$
R56	NN	$C + CD_2CN \rightarrow DC_3N + D$	$1.00 \times 10^{-10} \text{ cm}^3 \text{ s}^{-1}$
R57	NN	$C + CHDCN \rightarrow HC_3N + D$	$1.00 \times 10^{-10} \text{ cm}^3 \text{ s}^{-1}$
R58	NN	$N + C_2H_2D \rightarrow CHDCN + H$	$6.20 \times 10^{-11} \text{ cm}^3 \text{ s}^{-1}$
R59	CE	$H^+ + CD_2CN \rightarrow CD_2CN^+ + H$	$6.30 \times 10^{-09} \text{ cm}^3 \text{ s}^{-1}$
R60	CE	$C^+ + CD_2CN \rightarrow CD_2CN^+ + C$	$2.00 \times 10^{-09} \text{ cm}^3 \text{ s}^{-1}$
R61	CE	$H^+ + CH_2DCN \rightarrow CH_2DCN^+ + H$	$8.40 \times 10^{-09} \text{ cm}^3 \text{ s}^{-1}$
R62	CE	$O^+ + CH_2DCN \rightarrow CH_2DCN^+ + O$	$2.94 \times 10^{-09} \text{ cm}^3 \text{ s}^{-1}$
R63	CE	$H^+ + CHD_2CN \rightarrow CHD_2CN^+ + H$	$8.40 \times 10^{-09} \text{ cm}^3 \text{ s}^{-1}$
R64	CE	$O^+ + CHD_2CN \rightarrow CHD_2CN^+ + O$	$2.94 \times 10^{-09} \text{ cm}^3 \text{ s}^{-1}$
R65	CE	$H^+ + CHDCN \rightarrow CHDCN^+ + H$	$6.30 \times 10^{-09} \text{ cm}^3 \text{ s}^{-1}$
R66	CE	$C^+ + CHDCN \rightarrow CHDCN^+ + C$	$2.00 \times 10^{-09} \text{ cm}^3 \text{ s}^{-1}$
R67	DR	$CHD_2CN^+ + e^- \rightarrow CD_2CN + H$	$8.22 \times 10^{-07} \text{ cm}^3 \text{ s}^{-1}$
R68	DR	$CHD_2CNH^+ + e^- \rightarrow CD_2CN + H_2$	$8.22 \times 10^{-07} \text{ cm}^3 \text{ s}^{-1}$
R69	DR	$CD_2CN^+ + e^- \rightarrow CN + CD_2$	$8.22 \times 10^{-07} \text{ cm}^3 \text{ s}^{-1}$
R70	DR	$CD_2CN^+ + e^- \rightarrow DCN + CD$	$8.22 \times 10^{-07} \text{ cm}^3 \text{ s}^{-1}$
R71	DR	$CH_2DCNH^+ + e^- \rightarrow CH_2DCN + H$	$8.22 \times 10^{-07} \text{ cm}^3 \text{ s}^{-1}$
R72	DR	$CH_2DCN^+ + e^- \rightarrow DCN + CH_2$	$8.22 \times 10^{-07} \text{ cm}^3 \text{ s}^{-1}$
R73	DR	$CH_2DCN^+ + e^- \rightarrow CHDCN + H$	$8.22 \times 10^{-07} \text{ cm}^3 \text{ s}^{-1}$
R74	DR	$CHD_2CNH^+ + e^- \rightarrow CHD_2CN + H$	$8.22 \times 10^{-07} \text{ cm}^3 \text{ s}^{-1}$
R75	DR	$CHD_2CN^+ + e^- \rightarrow DCN + CHD$	$8.22 \times 10^{-07} \text{ cm}^3 \text{ s}^{-1}$
R76	DR	$CH_2DCNH^+ + e^- \rightarrow CHDCN + H_2$	$8.22 \times 10^{-07} \text{ cm}^3 \text{ s}^{-1}$
R77	DR	$CHDCN^+ + e^- \rightarrow CN + CHD$	$8.22 \times 10^{-07} \text{ cm}^3 \text{ s}^{-1}$
R78	DR	$CHDCN^+ + e^- \rightarrow DCN + CH$	$8.22 \times 10^{-07} \text{ cm}^3 \text{ s}^{-1}$
R79	PH	$CH_2DCN + PHOTON \rightarrow CH_2DCN^+ + e^-$	$2.13 \times 10^{-23} \text{ s}^{-1}$
R80	PH	$CH_2DCN + PHOTON \rightarrow CN + CH_2D$	$7.01 \times 10^{-18} \text{ s}^{-1}$
R81	PH	$CHD_2CN + PHOTON \rightarrow CHD_2CN^+ + e^-$	$2.13 \times 10^{-23} \text{ s}^{-1}$
R82	PH	$CHD_2CN + PHOTON \rightarrow CN + CHD_2$	$7.01 \times 10^{-18} \text{ s}^{-1}$

Reaction number	Reaction type	Reaction pathways for different isotopomers of Cyanomethyl radical	Rate coefficient at T=10K $A_V = 10$
R83	CRP	$CH_2DCN + CRPHOT \rightarrow CH_2DCN^+ + e^-$	$3.65 \times 10^{-14} s^{-1}$
R84	CRP	$CH_2DCN + CRPHOT \rightarrow CN + CH_2D$	$7.76 \times 10^{-14} s^{-1}$
R85	CRP	$CHD_2CN + CRPHOT \rightarrow CHD_2CN^+ + e^-$	$3.65 \times 10^{-17} s^{-1}$
R86	CRP	$CHD_2CN + CRPHOT \rightarrow CN + CHD_2$	$7.76 \times 10^{-14} s^{-1}$
R87	RA	$CH_2D + CN \rightarrow CH_2DCN + PHOTON$	$1.00 \times 10^{-16} cm^3 s^{-1}$
R88	RA	$CH_2D^+ + HCN \rightarrow CH_2DCNH + PHOTON$	$4.93 \times 10^{-08} cm^3 s^{-1}$
R89	RA	$CHD_2 + CN \rightarrow CHD_2CN + PHOTON$	$1.00 \times 10^{-16} cm^3 s^{-1}$
R90	RA	$CHD_2^+ + HCN \rightarrow CHD_2CNH^+ + PHOTON$	$4.93 \times 10^{-08} cm^3 s^{-1}$
R91	AD	$CH_2D + CN^- \rightarrow CH_2DCN + e^-$	$1.00 \times 10^{-09} cm^3 s^{-1}$
R92	AD	$CHD_2 + CN^- \rightarrow CHD_2CN + e^-$	$1.00 \times 10^{-09} cm^3 s^{-1}$
R93	REA	$CH_2CN + e^- \rightarrow CH_2CN^- + PHOTON$	$6.85 \times 10^{-7} cm^3 s^{-1}$
R94	REA	$CD_2CN + e^- \rightarrow CD_2CN^- + PHOTON$	$6.85 \times 10^{-7} cm^3 s^{-1}$
R95	REA	$CHDCN + e^- \rightarrow CHDCN^- + PHOTON$	$6.85 \times 10^{-7} cm^3 s^{-1}$
R96	MN	$CH_2CN^- + H_3^+ \rightarrow CH_2CN + H_2 + H$	$4.11 \times 10^{-7} cm^3 s^{-1}$
R97	MN	$CH_2CN^- + C^+ \rightarrow CH_2CN + C$	$4.11 \times 10^{-7} cm^3 s^{-1}$
R98	MN	$CH_2CN^- + H_3O^+ \rightarrow CH_2CN + H + H_2O$	$4.11 \times 10^{-7} cm^3 s^{-1}$
R99	MN	$CH_2CN^- + HCO^+ \rightarrow CH_2CN + H + CO$	$4.11 \times 10^{-7} cm^3 s^{-1}$
R100	MN	$CH_2CN^- + HN_2^+ \rightarrow CH_2CN + H + N_2$	$4.11 \times 10^{-7} cm^3 s^{-1}$
R101	MN	$CH_2CN^- + O^+ \rightarrow CH_2CN + O$	$4.11 \times 10^{-7} cm^3 s^{-1}$
R102	MN	$CH_2CN^- + H^+ \rightarrow CH_2CN + H$	$4.11 \times 10^{-7} cm^3 s^{-1}$
R103	MN	$CHDCN^- + H_3^+ \rightarrow CHDCN + H_2 + H$	$4.11 \times 10^{-7} cm^3 s^{-1}$
R104	MN	$CHDCN^- + C^+ \rightarrow CHDCN + C$	$4.11 \times 10^{-7} cm^3 s^{-1}$
R105	MN	$CHDCN^- + H_3O^+ \rightarrow CHDCN + H + H_2O$	$4.11 \times 10^{-7} cm^3 s^{-1}$
R106	MN	$CHDCN^- + HCO^+ \rightarrow CHDCN + H + CO$	$4.11 \times 10^{-7} cm^3 s^{-1}$
R107	MN	$CHDCN^- + HN_2^+ \rightarrow CHDCN + H + N_2$	$4.11 \times 10^{-7} cm^3 s^{-1}$
R108	MN	$CHDCN^- + O^+ \rightarrow CHDCN + O$	$4.11 \times 10^{-7} cm^3 s^{-1}$
R109	MN	$CHDCN^- + H^+ \rightarrow CHDCN + H$	$4.11 \times 10^{-7} cm^3 s^{-1}$
R110	MN	$CD_2CN^- + H_3^+ \rightarrow CD_2CN + H_2 + H$	$4.11 \times 10^{-7} cm^3 s^{-1}$
R111	MN	$CD_2CN^- + C^+ \rightarrow CD_2CN + C$	$4.11 \times 10^{-7} cm^3 s^{-1}$
R112	MN	$CD_2CN^- + H_3O^+ \rightarrow CD_2CN + H + H_2O$	$4.11 \times 10^{-7} cm^3 s^{-1}$
R113	MN	$CD_2CN^- + HCO^+ \rightarrow CD_2CN + H + CO$	$4.11 \times 10^{-7} cm^3 s^{-1}$
R114	MN	$CD_2CN^- + HN_2^+ \rightarrow CD_2CN + H + N_2$	$4.11 \times 10^{-7} cm^3 s^{-1}$
R115	MN	$CD_2CN^- + O^+ \rightarrow CD_2CN + O$	$4.11 \times 10^{-7} cm^3 s^{-1}$
R116	MN	$CD_2CN^- + H^+ \rightarrow CD_2CN + H$	$4.11 \times 10^{-7} cm^3 s^{-1}$

^a Polarizability of neutral reactants in units of A^3 and dipole moment in Debye (Woon & Herbst 2009)

Table A2. Initial abundances relative to the total hydrogen nuclei

Species	Abundance
H ₂	5.00×10^{-01}
He	1.00×10^{-01}
N	2.14×10^{-05}
O	1.76×10^{-04}
H ₃ ⁺	1.00×10^{-11}
C ⁺	7.30×10^{-05}
S ⁺	8.00×10^{-08}
Si ⁺	8.00×10^{-09}
Fe ⁺	3.00×10^{-09}
Na ⁺	2.00×10^{-09}
Mg ⁺	7.00×10^{-09}
P ⁺	3.00×10^{-09}
Cl ⁺	4.00×10^{-09}
e ⁻	7.31×10^{-05}
HD	1.6×10^{-05}

Chemical evolution and Deuterium enrichment:

Depending on the concentration of the gas phase species, all the neutral species (except H₂ and He) are allowed to accrete on the grain surface. Surface species are allowed to populate the gas phase by the thermal evaporation or cosmic ray induced evaporation processes. Initial elemental abundances have been chosen to be same as in Das et al. (2013b) and these are the typical low metal abundances often adopted for TMC-1 cloud. Initial elemental abundances are given in Table A2. Unless otherwise stated, for all the cases, we assume the initial abundance of HD to be 1.6×10^{-5} with respect to total hydrogen nuclei. This implies to the initial fractionation ratio (HD/H₂) 3.2×10^{-5} .

According to Palmeirim et al. (2013) and references therein, interstellar filaments could play a fundamental role in the star formation process. Taurus molecular cloud were known to exhibit large scale filamentary structure long before the Herschel (Schneider & Elmegreen 1979; Goldsmith et al. 2008). TMC-1 has recently been mapped with Herschel (Pilbratt et al. 2010) as a part of the Gould Belt Survey (Andre et al. 2010). Results obtained from the Herschel Gould Belt survey confirm the omnipresence of parsec scale filaments in nearby molecular clouds and suggest that the observed filamentary structure is directly related to the formation of prestellar cores. Herschel observations now demonstrate that filaments are truly ubiquitous in the cold interstellar medium (ISM). Palmeirim et al. (2013) made an attempt to prepare an analytical model for an idealized cylindrical filament. As per their model, filament will have dense, flat inner portion and have a power law behaviour at the larger radii. They assumed the Plummer-like function (Nutter et al., 2008; Arzoumanian et al., 2011) for the density profile;

$$\rho_p(r) = \rho_c / [1 + (r/R_{flat})^2]^{p/2} \rightarrow N(r) = A_p \frac{\rho_c R_{flat}}{[1 + (r/R_{flat})^2]^{(p-1)/2}},$$

where, ρ_c is the central density, R_{flat} is the size of the flat inner part, parameter p defines the steepness of the profile in the outer part, A_p is a finite factor which controls filament's inclination angle to the plane of sky. As per Ostriker (1964), the density structure of an isothermal gas cylinder in hydrostatic equilibrium could follow above equation with $p = 4$. In order to start with

a simple realistic physical condition for TMC-1 cloud, we have considered different regions of the cloud possessing different values of visual extinction parameter (A_V). Lee et al., (1996) assumed a static, plane parallel, semi infinite cloud with a constant temperature 30K and a density profile to mimic the condition of a self gravitating isothermal sphere. Following relation was considered by them:

$$n_H = n_{H0}/(1 - cr/r_{max})^2,$$

where, $n_H = n(H) + 2n(H_2)$ is the number density of the hydrogen nuclei in the units of cm^{-3} , n_{H0} is the cloud density at the cloud surface, n_{Hmax} is the maximum number density, r_{max} is the maximum cloud depth, n_{H0} is the hydrogen density at the cloud surface ($r=0$) and c is a constant. By evaluating the constant c , they derived the following relationship between the hydrogen number density and the visual extinction parameter:

$$n_H = n_{H0} \left[1 + \left[\left(\frac{n_{Hmax}}{n_{H0}} \right)^{1/2} - 1 \right] \frac{A_V}{A_{Vmax}} \right]^2, \quad (11)$$

A_{Vmax} is the maximum visual extinction considered very deep inside the cloud. Lee et al. (1996) considered above relationship for $T = 30\text{K}$, $n_{H0} = 1 \times 10^2 \text{ cm}^{-3}$, $n_{Hmax} = 1.042 \times 10^4 \text{ cm}^{-3}$, $A_{Vmax} = 10.86$. As in Das & Chakrabarti (2011), in the present simulation, we assume that this relationship also holds for $T=10\text{K}$. Values of n_{H0} , n_{Hmax} and A_{Vmax} are assumed to be similar to the values assumed by Lee et al. (1996).

In Fig. A1.(a-f), we show chemical evolution of different forms of cyanomethyl radical and some of its related molecules. We have considered $A_V = 10$, which corresponds to a hydrogen number density of $(n_H) = 8984.52 \text{ cm}^{-3}$. Due to the huge abundances of hydrogenated species, abundances of any interstellar species are normally described with respect to the total number of hydrogen or with respect to the hydrogen molecule. In our case, we have presented the chemical abundances with respect to the total hydrogen nuclei in all forms. From the past observations, it is now known that water, Methanol and Carbon-di oxide are the major constituents of the interstellar grain mantle. According to Tielens et al. (1991), the abundance of water around the dense cloud region in the ice phase is $\sim 10^{-4}$ and according to Das, Acharyya & Chakrabarti (2010) and references therein, abundances of CO_2 and methanol in the ice phase could vary between 5-20% and 2-30% respectively with respect to the solid state water. These huge abundances could be manifested in the gas phase through some interstellar energetic events. Recent observational facility, such as the Atacama Large Millimeter/submillimeter Array (ALMA) could be very useful for the confirmed detection of the interstellar complex species having magnitudes $\sim 10^{10}$ times lower than the Water molecules. Most of the molecules in Fig. A1 attain a peak value near $\sim 10^5$ years. In Fig. A1.a, different forms of neutral CH_2CN are shown and it is evident that all the deuterated forms of CH_2CN are reasonably abundant (peak abundance $> 10^{-14}$ with respect to n_H). In Fig. A1.b, the chemical evolution of CH_2CN^- and its two deuterated isotopomers are shown. Different forms of these molecules are also reasonably abundant (peak abundances $> 10^{-13}$ with respect to n_H). Chemical evolution of CH_2CN^+ and two of its deuterated isotopomers are shown in Fig. A1.c. Deuterated isotopomers of CH_2CN^+ are not very

abundant (peak abundances $> 10^{-15}$ with respect to n_H). In Fig. A1.d, the chemical evolution of CH_3CN along with its two deuterated isotopomers and chemical evolution of HCN and DCN are shown. All of them are found to be abundant (peak abundances $> 10^{-13}$ with respect to n_H). Chemical evolution of CH_3CN^+ along with its two deuterated isotopomers are shown in Fig. A1.e. Abundances of these species are several orders lower than the present observational limit. Figure 3f shows the chemical evolutions of CH_3CNH^+ ion and its two deuterated isotopomers. Deuterated isotopomers of this ion are not very abundant. In brief, from Fig. A1, it is evident that various forms of CH_2CN^- are reasonably abundant and could be observed with the present observational facility. In order to justify our modeling results, in Table A3, we have compared our calculated abundances of some related species of the cyanomethyl anions with the existing theoretical/observational results.

In Table A4, we have presented peak column densities of all the species for $A_V=1$ ($n_H = 341.46 \text{ cm}^{-3}$), 5 ($n_H = 2745.07 \text{ cm}^{-3}$) and 10 ($n_H = 8984.52 \text{ cm}^{-3}$). Column densities of the species are computed by following the relationship developed by Shalabiea et al. (1994):

$$N(A) = n_H x_i R, \quad (12)$$

where, n_H is the total hydrogen number density, x_i is the abundance of the i^{th} species and R is the path length along the line of sight ($= \frac{1.6 \times 10^{21} \times A_V}{n_H}$). From Table A4, it is evident that the column density of all the species are increasing linearly up to the intermediate region ($A_V=5$ and $n_H = 2745.07 \text{ cm}^{-3}$) of the cloud and beyond that the column density of all the species increases very slowly. From Table A4, it is evident that CH_2CN^- along with its deuterated isotopomers are the most abundant and require detail spectral studies to observe them in or around ISMs.

Despite the low elemental D/H ratio ($\sim 10^{-5}$, Linsky et al. 1995), several molecules in the interstellar medium are found to be heavily fractionated. In our simulation, we vary the initial fractionation ratio to check the fractionation of CH_2CN^- . To mimic the physical condition, we have considered $A_V = 10$, $n_H = 8984.52 \text{ cm}^{-3}$ and $T=10\text{K}$ for this case. Fractionation ratio of the CH_2CN^- attaining a peak value near the intermediate time scale. In Fig. A2, only the peak values of the fractionation ratio is shown for different initial fractionation ratio. We have also checked the fractionation ratios for CH_2CN and CH_2CN^+ and found that they behave in the same way as CH_2CN^- (fractionation values are also very similar). It is interesting to note that the fractionation ratio for the singly deuterated cyanomethyl anion often crosses the elemental D/H ratio. For the doubly deuterated isotopomer, the fractionation ratio crosses the elemental D/H ratio for an initial fractionation ratio $> 10^{-5}$.

Table A3. Comparison of fractional abundances with other observations/models.

Species	Fractional abundance by observations/other chemical models	Fractional abundance by our model ^C	
		Peak abundance	Abundance after 2×10^6 year
CH ₂ CN	2.5×10^{-09O} , 4.59×10^{-11W}	1.46×10^{-09}	1.43×10^{-11}
CH ₃ CN	5.00×10^{-10O} , 6.95×10^{-12W}	5.01×10^{-09}	3.74×10^{-13}
HCN	1.00×10^{-08O} , 2.95×10^{-9W}	4.93×10^{-08}	9.01×10^{-10}
CH ₃ CN ⁺	1.02×10^{-18W}	6.24×10^{-16}	3.49×10^{-19}
CH ₃ CNH ⁺	2.55×10^{-14W}	2.78×10^{-10}	5.36×10^{-17}
DCN	$2.1 - 3.7 \times 10^{-10T}$	1.38×10^{-07}	2.69×10^{-10}

^O Observation by Ohishi, Irvine & Kaifu (1992) in TMC-1.
^W Chemical model by Woodall et al. (2007), by considering $n_H = 2 \times 10^4 \text{ cm}^{-3}$, $T = 10K$, $A_V = 15$
^T Observation by Turner (2001) in TMC-1.
^C Our model by considering $n_H = 8984.52 \text{ cm}^{-3}$, $T = 10K$, $A_V = 10$.

Table A4. Column densities of various forms of CH₂CN and its related molecules around different regions of the ISM.

Species	Isotopomers	AV ₁	AV ₅	AV ₁₀
		($n_H = 341.46 \text{ cm}^{-3}$)	($n_H = 2745.07 \text{ cm}^{-3}$)	($n_H = 8984.52 \text{ cm}^{-3}$)
CH ₂ CN	CH ₂ CN	2.11×10^{07}	1.10×10^{13}	2.33×10^{13}
	CHDCN	8.76×10^{02}	4.95×10^{11}	1.21×10^{12}
	CD ₂ CN	4.69×10^{-02}	3.89×10^{09}	1.44×10^{10}
CH ₂ CN ⁻	CH ₂ CN ⁻	3.52×10^{07}	4.35×10^{13}	4.91×10^{13}
	CHDCN ⁻	1.46×10^{03}	1.04×10^{12}	9.43×10^{11}
	CD ₂ CN ⁻	7.85×10^{-02}	6.03×10^{09}	5.99×10^{09}
CH ₂ CN ⁺	CH ₂ CN ⁺	2.76×10^{04}	2.42×10^{11}	4.67×10^{12}
	CHDCN ⁺	1.99×10^{01}	1.09×10^{11}	2.34×10^{12}
	CD ₂ CN ⁺	1.05×10^{-03}	9.88×10^{08}	2.56×10^{10}
CH ₃ CN	CH ₃ CN	1.38×10^{05}	2.59×10^{13}	8.02×10^{13}
	CH ₂ DCN	9.42×10^{01}	6.81×10^{11}	1.64×10^{12}
	CHD ₂ CN	5.05×10^{-03}	5.12×10^{09}	1.81×10^{10}
CH ₃ CN ⁺	CH ₃ CN ⁺	4.67×10^{02}	4.08×10^{06}	9.99×10^{06}
	CH ₂ DCN ⁺	1.73×10^{-02}	3.03×10^{05}	2.49×10^{05}
	CHD ₂ CN ⁺	9.58×10^{-07}	2.43×10^{03}	5.00×10^{03}
CH ₃ CNH ⁺	CH ₃ CNH ⁺	4.28×10^{03}	3.31×10^{11}	4.44×10^{12}
	CHDCNH ⁺	2.31×10^{00}	2.27×10^{10}	3.18×10^{11}
	CD ₃ CNH ⁺	1.24×10^{-04}	2.24×10^{08}	4.10×10^{09}
HCN	HCN	5.66×10^{10}	6.09×10^{14}	7.88×10^{14}
	DCN	2.23×10^{12}	2.61×10^{15}	2.20×10^{15}

Appendix B

Species name	Charge	Spin state	Peak positions (Gas phase) (Wavenumber in cm^{-1})	Absorbance	Peak positions (H_2O ice) (Wavenumber in cm^{-1})	Absorbance	
CH_2CN	Neutral	Doublet	380.17	0.01	385.95	0.05	
			422.18	0.14	428.20	0.0002	
			741.27	71.00	751.76	93.08	
			1056.15	6.08	1053.51	8.59	
			1063.44	0.006	1058.47	0.14	
			1466.41	6.00	1449.31	12.60	
			2053.44	0.2927	2059.24	10.1890	
			3146.77	0.079	3151.71	1.10	
			3253.38	0.01	3261.55	1.29	
		Quartet	401.64	3.42	406.18	7.018	
			556.11	8.80	548.63	12.04	
			875.41	8.60	881.00	14.6476	
			879.36	65.39	887.16	86.94	
			1104.57	12.98	1116.92	15.47	
			1296.70	11.87	1295.95	30.54	
			1456.34	20.54	1441.09	37.11	
			3052.49	1.00	3054.17	5.09	
		3186.69	1.70	3185.07	4.62		
		Sextet	346.18	10.91	345.31	18.83	
			428.48	1.42	433.95	1.88	
			608.07	23.39	605.39	24.95	
			705.71	53.97	699.05	103.80	
			958.65	2.94	958.74	5.04	
			1080.66	35.15	1082.93	58.80	
			1448.14	3.18	1435.41	5.81	
			3046.08	8.38	3051.37	5.48	
			3144.26	10.31	3152.23	8.39	
		Cation	Singlet	332.70	1.80	333.41	1.11
				361.52	3.38	347.41	2.37
				1065.83	0.007	1055.97	0.12
1098.41	59.90			1088.41	130.90		
1190.97	11.68			1206.97	10.25		
1472.11	12.54			1444.50	10.20		
2166.72	337.15			2188.75	429.60		
3072.41	45.84			3111.38	54.35		
3182.95	62.98			3225.45	77.92		
Triplet	297.90		3.08	288.14	0.54		
	367.58		1.02	370.92	0.93		
	769.81		76.01	748.11	103.45		
	795.38		97.74	767.54	113.28		
1071.82	0.72	1085.46	0.01				
1258.22	190.80	1202.05	301.70				
1633.10	0.56	1671.14	2.36				
2966.42	359.92	2985.29	533.60				
3018.48	212.29	3042.26	258.24				

Species name	Charge	Spin state	Peak positions (Gas phase) (Wavenumber in cm^{-1})	Absorbance	Peak positions (H_2O ice) (Wavenumber in cm^{-1})	Absorbance
		Quintet	346.84 462.66 753.89 949.30 1028.76 1317.33 1444.11 3050.21 3174.04	5.33 1.00 11.34 57.41 1.00 16.46 72.83 92.34 55.18	349.97 483.27 774.18 966.14 1039.23 1345.83 1439.88 3087.88 3209.66	7.44 2.29 16.94 65.41 5.06 14.82 112.56 106.8981 57.81
		Singlet	359.32 (343.2 ^f) 414.56 (434.5 ^f) 533.07 (585.5 ^f) 1048.07 (1045.5 ^f) 1075.67 (991.5 ^f) 1444.91 (1298.2 ^f) 2056.73 (2115.7 ^f) 3112.82 (3122.3 ^f) 3190.46 (3191.3 ^f)	327.78 2.55 10.77 0.26 16.93 11.31 673.64 15.15 51.00	352.23 415.95 532.56 1044.80 1088.82 1436.32 2016.35 3124.48 3208.80	557.70 3.02 12.91 0.83 26.07 34.49 1451.74 3.64 25.05
	Anion	Triplet	267.97 380.97 724.28 998.59 1029.93 1414.96 2047.42 3004.22 3075.31	97.84 120.36 648.90 686.60 22.97 880.97 12.02 8.9511 426.77	230.03 327.49 710.95 983.77 1008.78 1345.70 2041.51 2854.88 3344.74	270.80 44100.90 470.37 10158.64 149.60 3023.70 509.41 1248.3729 430118.36
		Quintet	380.69 528.98 848.23 866.53 1093.33 1300.64 1413.46 2943.40 3053.47	55.85 254.03 248.93 1075.23 264.32 242.77 487.14 21.20 115.4081	377.65 470.96 530.66 780.28 923.99 1139.37 1429.66 2958.33 3006.99	52.17 36.07 95.05 43.80 1.48 89.16 5.21 161.83 128.18

Species name	Charge	Spin state	Peak positions (Gas phase) (Wavenumber in cm^{-1})	Absorbance	Peak positions (H_2O ice) (Wavenumber in cm^{-1})	Absorbance
CHDCN	Neutral	Doublet	360.12	0.0305	364.81	0.3103
			414.01	0.3487	420.29	0.0622
			674.97	53.6634	683.66	70.3703
			894.49	1.8954	892.34	2.8317
			1055.05	4.7613	1052.14	6.7508
			1337.89	3.2483	1322.47	7.1377
			2052.21	0.2364	2058.10	10.4464
			2349.18	0.2326	2353.90	0.4898
		3204.29	0.0384	3211.04	1.2018	
		Quartet	367.00	3.26	371.42	6.71
			508.89	3.61	503.27	5.62
			796.55	62.02	803.16	81.68
			805.91	4.28	807.13	8.06
			1046.16	11.57	1060.44	12.96
			1240.95	21.08	1240.38	43.42
			1375.51	13.01	1364.19	23.7859
			2250.01	0.33	2252.38	1.90
		3171.93	2.37	3169.75	7.63	
		Sextet	316.41	8.3996	317.46	14.4958
			380.63	3.5056	383.53	5.4820
			584.05	27.9405	586.27	34.1346
			679.35	33.6185	670.45	70.1195
			808.06	3.2080	807.46	4.9155
			1072.42	33.7646	1075.20	56.6412
			1307.13	3.5049	1296.24	6.9014
			2266.78	4.3870	2271.75	3.0207
		3098.56	9.4154	3105.36	7.0616	
		Cation	Singlet	327.28	1.0415	328.67
	342.81			1.4710	330.06	0.6979
	896.55			8.7921	891.23	15.5052
	1080.99			5.3437	1080.71	109.5207
	1090.64			50.2969	1095.07	4.1450
	1347.18			2.6195	1321.79	0.9668
	2156.55			336.6641	2181.29	427.8153
	2308.93			9.8690	2335.43	11.3447
	3132.20			55.7510	3173.15	67.9790
	Triplet			279.82	3.4254	268.24
			362.00	0.9464	364.66	0.9042
			676.34	53.8833	671.54	74.4633
			720.96	68.9088	696.44	80.0691
1042.19			15.2728	1034.36	91.3915	
1143.64			136.3938	1112.61	146.0176	
1624.63			0.2071	1662.24	0.6087	
2198.34			159.8451	2213.71	227.5224	
2992.93			287.4476	3014.33	396.0676	
Quintet	336.09		5.50	340.23	7.70	
	377.56		1.71	394.24	3.08	
	691.98		8.97	707.33	14.13	
	882.81		46.11	894.99	53.63	
	945.72		0.48	957.60	2.50	
	1245.25		0.46	1252.44	5.20	
	1360.00	72.87	1380.17	102.28		
	2302.28	47.10	2323.43	53.74		
	3092.36	64.05	3136.19	73.83		

Species name	Charge	Spin state	Peak positions (Gas phase) (Wavenumber in cm^{-1})	Absorbance	Peak positions (H_2O ice) (Wavenumber in cm^{-1})	Absorbance
	Anion	Singlet	320.38	265.9975	315.18	445.8616
			390.54	2.0832	391.19	2.7553
			532.73	14.1738	531.43	22.1992
			890.57	0.7390	890.03	1.0047
			1068.77	14.2137	1079.21	20.9991
			1320.07	13.3165	1314.13	35.9126
			2053.96	671.4335	2013.34	1438.5730
			2314.43	10.3086	2326.47	15.7194
		3153.96	34.8815	3169.35	15.4877	
		Triplet	256.03	73.2647	224.97	257.8315
			373.69	126.5104	315.27	40032.8173
			659.32	447.5905	649.24	314.4611
			838.42	533.0538	815.96	13084.5480
			1022.75	106.1802	1002.20	1273.5056
			1286.26	690.3204	1229.75	2932.2540
			2045.45	8.9107	2038.72	1030.7865
			2239.84	41.39	2228.67	43853.1197
		3042.11	231.0028	3157.93	283695.8348	
		Quintet	362.33	66.32	324.83	48.00
			429.86	212.83	425.17	23.09
			739.90	194.13	516.60	74.48
			810.32	587.01	772.71	23.19
			1082.59	127.96	791.52	20.15
			1199.89	567.59	1124.15	79.07
			1351.70	91.59	1295.14	11.46
			2193.92	37.333	2184.96	84.31
		3012.36	52.63	2983.33	143.03	
		CD_2CN	Neutral	Doublet	344.40	0.13
397.78	0.80				404.60	0.34
606.56	36.40				613.17	48.00
870.49	0.24				869.34	0.02
937.96	7.22				934.57	11.69
1168.69	0.03				1156.60	0.27
2050.54	0.18				2056.49	10.54
2283.18	0.16				2286.56	0.88
2424.21	0.30			2430.64	0.09	
Quartet	356.14			3.08	360.18	6.23
	436.96			5.69	431.70	7.60
	705.79			32.37	712.16	41.85
	745.87			4.23	746.78	8.19
	1000.62			3.80	995.42	9.63
	1080.21			25.93	1097.22	37.52
	1335.61			7.67	1329.22	17.85
	2221.86			1.00	2222.68	4.01
2362.52	1.00			2361.63	1.27	
Sextet	312.60			10.55	312.88	17.72
	325.59			1.00	329.88	1.00
	534.81			29.10	536.76	40.18
	666.20			18.03	652.36	42.20
	750.05			1.27	750.38	2.18
	998.80			17.51	996.79	24.84
	1129.20			19.14	1123.54	37.91
	2201.52			2.88	2205.59	1.35
2339.01	6.03			2345.20	4.96	

Species name	Charge	Spin state	Peak positions (Gas phase) (Wavenumber in cm^{-1})	Absorbance	Peak positions (H_2O ice) (Wavenumber in cm^{-1})	Absorbance	
		Singlet	318.34	0.2651	316.60	0.0929	
			328.26	0.5487	320.36	0.0361	
			869.40	1.8879	866.28	1.1613	
			950.70	39.7773	940.72	75.7327	
			959.62	0.9499	970.72	0.3826	
			1201.42	9.0447	1180.60	33.1407	
			2137.45	307.90	2166.38	394.2006	
			2261.07	28.5996	2282.02	30.7198	
			2374.60	20.7168	2405.56	26.2027	
		Cation	Triplet	265.88	3.7658	316.60	0.0929
				351.80	0.7345	320.36	0.0361
				640.54	41.4409	866.28	1.1613
				643.21	49.7048	940.72	75.7327
				881.69	52.4016	970.72	0.3826
				1086.73	41.6529	1180.60	33.1407
				1615.46	0.9962	2166.38	394.2006
				2164.45	206.2750	2282.02	30.7198
				2234.00	114.3264	2405.56	26.2027
		Quintet	315.20	4.46	318.61	6.56	
			362.42	1.21	377.86	2.41	
			680.50	8.55	695.04	12.83	
			759.64	24.26	772.30	27.80	
			900.04	2.38	908.44	6.94	
			1037.39	3.00	1036.94	4.41	
			1330.49	54.80	1359.99	78.72	
			2214.89	60.13	2241.36	70.72	
			2363.00	21.62	2390.47	23.87	
		Anion	Singlet	277.57	204.9094	272.73	334.5490
				372.18	1.7243	372.41	2.5120
				532.47	16.9905	530.58	30.9795
866.57	0.8907			866.50	1.3089		
942.63	1.5371			942.87	0.7288		
1167.74	25.6880			1173.99	53.0751		
2050.23	663.9194			2009.48	1413.2486		
2261.10	6.7069			2271.46	34.4696		
2373.80	22.5826			2388.17	10.7051		
Triplet	246.64		56.9436	216.52	235.1422		
	360.02		130.5705	305.25	36839.6098		
	591.20		250.5390	581.93	169.2967		
	802.93		597.9890	784.05	18556.8130		
	915.87		187.5826	881.66	901.8334		
	1122.78		269.6364	1084.62	675.4565		
	2042.43		6.3038	2025.21	1008.1370		
	2188.64		1.7398	2095.03	220.3006		
	2296.73		111.0626	2488.81	224264.5837		
	Quintet		334.90	65.68	311.27	56.61	
			416.91	189.14	354.95	15.50	
			698.46	468.08	487.92	35.46	
			721.28	189.17	731.91	0.50	
			974.96	442.26	777.68	38.81	
			1084.64	62.26	1001.84	24.61	
			1327.22	16.20	1172.44	63.76	
			2145.27	5.14	2138.82	99.02	
			2264.94	73.69	2232.85	66.07	
^f Computed vibrational (harmonic) frequencies by Fortenberry, Crawford & Lee (2013)							

Table B2. Rotational transitions for gas phase CH_2CN^- by considering the experimental values of the spectroscopic constants. Errors on the computed line frequencies are related to the errors on the constants given in Table 2 and from there, the error (dv/v) on any line frequency for CH_2CN^- is found to be $= 6.16 \times 10^{-5}$.

Frequency (in MHz)	I^c	D^d	E_{lower}^e (in cm^{-1})	g_{up}^f	QnF^h	Upper state (Qn_{up}^i)	Lower state (Qn_{lower}^j)
19950.2455	-6.1365	3	-0.0000	3	304	1 0 1 1	0 0 0 1
19950.9319	-5.9147	3	-0.0000	5	304	1 0 1 2	0 0 0 1
19951.9617	-6.6136	3	-0.0000	1	304	1 0 1 0	0 0 0 1
39900.8618	-5.8376	3	0.6655	5	304	2 0 2 2	1 0 1 2
39900.9762	-5.7126	3	0.6655	3	304	2 0 2 1	1 0 1 0
39901.5483	-5.3605	3	0.6655	5	304	2 0 2 2	1 0 1 1
39901.5973	-5.0894	3	0.6655	7	304	2 0 2 3	1 0 1 2
39902.6924	-5.8376	3	0.6655	3	304	2 0 2 1	1 0 1 1
59851.3698	-5.6650	3	1.9965	7	304	3 0 3 3	2 0 2 3
59851.9909	-4.9326	3	1.9965	5	304	3 0 3 2	2 0 2 1
59852.1053	-4.7619	3	1.9964	7	304	3 0 3 3	2 0 2 2
59852.1326	-4.6016	3	1.9965	9	304	3 0 3 4	2 0 2 3
59853.1351	-5.6649	3	1.9964	5	304	3 0 3 2	2 0 2 2
79801.6393	-5.5449	3	3.9929	9	304	4 0 4 4	3 0 3 4
79802.3530	-4.4869	3	3.9929	7	304	4 0 4 3	3 0 3 2
79802.4020	-4.3688	3	3.9929	9	304	4 0 4 4	3 0 3 3
79802.4193	-4.2536	3	3.9929	11	304	4 0 4 5	3 0 3 4
79803.3827	-5.5449	3	3.9929	7	304	4 0 4 3	3 0 3 3
99751.5713	-5.4542	3	6.6548	11	304	5 0 5 5	4 0 4 5
99752.3242	-4.1654	3	6.6548	9	304	5 0 5 4	4 0 4 3
99752.3514	-4.0740	3	6.6548	11	304	5 0 5 5	4 0 4 4
99752.3634	-3.9837	3	6.6548	13	304	5 0 5 6	4 0 4 5
99753.3049	-5.4542	3	6.6548	9	304	5 0 5 4	4 0 4 4
119701.0747	-5.3826	3	9.9822	13	304	6 0 6 6	5 0 5 6
119701.8494	-3.9135	3	9.9822	11	304	6 0 6 5	5 0 5 4
119701.8668	-3.8386	3	9.9822	13	304	6 0 6 6	5 0 5 5
119701.8756	-3.7642	3	9.9822	15	304	6 0 6 7	5 0 5 6
119702.8029	-5.3826	3	9.9822	11	304	6 0 6 5	5 0 5 5
139650.0604	-5.3247	3	13.9750	15	304	7 0 7 7	6 0 6 7
139650.8493	-3.7071	3	13.9750	13	304	7 0 7 6	6 0 6 5
139650.8613	-3.6435	3	13.9750	15	304	7 0 7 7	6 0 6 6
139650.8680	-3.5802	3	13.9750	17	304	7 0 7 8	6 0 6 7
139651.7854	-5.3247	3	13.9750	13	304	7 0 7 6	6 0 6 6
159598.4405	-5.2771	3	18.6333	17	304	8 0 8 8	7 0 7 8
159599.2393	-3.5331	3	18.6333	15	304	8 0 8 7	7 0 7 6
159599.2481	-3.4778	3	18.6333	17	304	8 0 8 8	7 0 7 7
159599.2534	-3.4226	3	18.6333	19	304	8 0 8 9	7 0 7 8
159600.1634	-5.2771	3	18.6333	15	304	8 0 8 7	7 0 7 7
179546.1275	-5.2378	3	23.9570	19	304	9 0 9 9	8 0 8 9
179546.9337	-3.3836	3	23.9570	17	304	9 0 9 8	8 0 8 7
179546.9404	-3.3347	3	23.9569	19	304	9 0 9 9	8 0 8 8
179546.9447	-3.2858	3	23.9570	21	304	9 0 9 10	8 0 8 9
179547.8490	-5.2378	3	23.9569	17	304	9 0 9 8	8 0 8 8
199493.0342	-5.2052	3	29.9460	21	304	10 0 10 10	9 0 9 10
199493.8461	-3.2535	3	29.9460	19	304	10 0 10 9	9 0 9 8
199493.8514	-3.2095	3	29.9460	21	304	10 0 10 10	9 0 9 9
199493.8550	-3.1657	3	29.9460	23	304	10 0 10 11	9 0 9 10
199494.7547	-5.2052	3	29.9460	19	304	10 0 10 9	9 0 9 9
219439.0735	-5.1783	3	36.6004	23	304	11 0 11 11	10 0 10 11
219439.8900	-3.1390	3	36.6004	21	304	11 0 11 10	10 0 10 9
219439.8943	-3.0992	3	36.6004	23	304	11 0 11 11	10 0 10 10

219439.8973	-3.0593	3	36.6004	25	304	11 01112	10 01011
219440.7933	-5.1783	3	36.6004	21	304	11 01110	10 01010
239384.1585	-5.1565	3	43.9201	25	304	12 01212	11 01112
239384.9787	-3.0377	3	43.9201	23	304	12 01211	11 01110
239384.9823	-3.0012	3	43.9201	25	304	12 01212	11 01111
239384.9848	-2.9647	3	43.9201	27	304	12 01213	11 01112
239385.8777	-5.1565	3	43.9201	23	304	12 01211	11 01111
259328.2022	-5.1391	3	51.9051	27	304	13 01313	12 01213
259329.0255	-2.9474	3	51.9051	25	304	13 01312	12 01211
259329.0285	-2.9138	3	51.9051	27	304	13 01313	12 01212
259329.0307	-2.8802	3	51.9051	29	304	13 01314	12 01213
259329.9209	-5.1391	3	51.9051	25	304	13 01312	12 01212
279271.1177	-5.1256	3	60.5554	29	304	14 01414	13 01314
279271.9437	-2.8668	3	60.5554	27	304	14 01413	13 01312
279271.9462	-2.8356	3	60.5554	29	304	14 01414	13 01313
279271.9481	-2.8044	3	60.5554	31	304	14 01415	13 01314
279272.8361	-5.1256	3	60.5554	27	304	14 01413	13 01313
299212.8181	-5.1158	3	69.8709	31	304	15 01515	14 01415
299213.6463	-2.7946	3	69.8709	29	304	15 01514	14 01413
299213.6485	-2.7655	3	69.8709	31	304	15 01515	14 01414
299214.5362	-5.1158	3	69.8709	29	304	15 01514	14 01414
319154.0468	-2.7300	3	79.8516	31	304	16 01615	15 01514
319154.9344	-5.1092	3	79.8516	31	304	16 01615	15 01515

¹ ^c Base 10 logarithm of the integrated intensity at 300K in nm² MHz

^d Degrees of freedom in the rotational partition function (0 for atoms, 2 for linear molecules, 3 for non linear molecules)

^e Lower state energy in cm⁻¹ relative to the lowest energy level in the ground vibronic state.

^f Upper state degeneracy : $g_{up} = g_l \times g_N$, where g_l is the spin statistical weight and $g_N = 2N + 1$ the rotational degeneracy.

^g Molecule Tag

^h Coding for the format of quantum numbers. $QnF=100 \times Q + 10 \times H + N_{Qn}$; N_{Qn} is the number of quantum numbers for each state; H indicates the number of half integer quantum numbers; $Q \bmod 5$, the residual when Q is divided by 5, gives the number of principal quantum numbers (without the spin designating ones).

ⁱ Quantum numbers for the upper state

^j Quantum numbers for the lower state

Table B3. Computed rotational transitions for gas phase CHDCN^- by considering our calculated values of spectroscopic constants. Since there are no experimentally fitted rotational and distortional constants available, we are only providing the line frequencies based on our theoretically calculated spectroscopic constants which are given in Table 2.

Frequency (in MHz)	F^c	D^d	E_{lower}^e	g_{up}^f	QnF^{gh}	Upper state (Qn_{up}^i)	Lower state (Qn_{lower}^j)
18477.4689	-6.2141	3	-0.0000	5	305	1 0 1 1 2	0 0 0 1 2
18478.1537	-5.9430	3	-0.0000	7	305	1 0 1 2 3	0 0 0 1 2
36955.3164	-5.9169	3	0.6164	7	305	2 0 2 2 3	1 0 1 2 3
36955.4305	-5.6651	3	0.6164	5	305	2 0 2 1 2	1 0 1 0 1
36956.0012	-5.3887	3	0.6163	7	305	2 0 2 2 3	1 0 1 1 2
36956.0501	-5.1546	3	0.6164	9	305	2 0 2 3 4	1 0 1 2 3
36957.1425	-5.9150	3	0.6163	5	305	2 0 2 1 2	1 0 1 1 2
55433.0730	-5.7579	3	1.8491	9	305	3 0 3 3 4	2 0 2 3 4
55433.6926	-4.9605	3	1.8491	7	305	3 0 3 2 3	2 0 2 1 2
55433.8067	-4.8268	3	1.8491	9	305	3 0 3 3 4	2 0 2 2 3
55433.8339	-4.6885	3	1.8491	11	305	3 0 3 4 5	2 0 2 3 4
55434.8339	-5.7440	3	1.8491	7	305	3 0 3 2 3	2 0 2 2 3
73910.6172	-5.6492	3	3.6982	11	305	4 0 4 4 5	3 0 3 4 5
73911.3292	-4.5514	3	3.6982	9	305	4 0 4 3 4	3 0 3 2 3
73911.3781	-4.4553	3	3.6981	11	305	4 0 4 4 5	3 0 3 3 4
73911.3954	-4.3548	3	3.6982	13	305	4 0 4 5 6	3 0 3 4 5
73912.3565	-5.6375	3	3.6981	9	305	4 0 4 3 4	3 0 3 3 4
92387.8593	-5.5671	3	6.1636	13	305	5 0 5 5 6	4 0 4 5 6
92388.6103	-4.2515	3	6.1636	11	305	5 0 5 4 5	4 0 4 3 4
92388.6375	-4.1747	3	6.1636	13	305	5 0 5 5 6	4 0 4 4 5
92388.6495	-4.0948	3	6.1636	15	305	5 0 5 6 7	4 0 4 5 6
92389.5886	-5.5580	3	6.1636	11	305	5 0 5 4 5	4 0 4 4 5
110864.7166	-5.5021	3	9.2453	15	305	6 0 6 6 7	5 0 5 6 7
110865.4895	-4.0136	3	9.2453	13	305	6 0 6 5 6	5 0 5 4 5
110865.5067	-3.9491	3	9.2453	15	305	6 0 6 6 7	5 0 5 5 6
110865.5155	-3.8825	3	9.2453	17	305	6 0 6 7 8	5 0 5 6 7
110866.4406	-5.4950	3	9.2453	13	305	6 0 6 5 6	5 0 5 5 6
129341.1089	-5.4492	3	12.9434	17	305	7 0 7 7 8	6 0 6 7 8
129341.8959	-3.8169	3	12.9434	15	305	7 0 7 6 7	6 0 6 5 6
129341.9078	-3.7611	3	12.9434	17	305	7 0 7 7 8	6 0 6 6 7
129341.9146	-3.7039	3	12.9434	19	305	7 0 7 8 9	6 0 6 7 8
129342.8297	-5.4435	3	12.9434	15	305	7 0 7 6 7	6 0 6 6 7
147816.9571	-5.4055	3	17.2578	19	305	8 0 8 8 9	7 0 7 8 9
147817.7540	-3.6500	3	17.2578	17	305	8 0 8 7 8	7 0 7 6 7
147817.7628	-3.6007	3	17.2578	19	305	8 0 8 8 9	7 0 7 7 8
147817.7681	-3.5504	3	17.2578	21	305	8 0 8 9 10	7 0 7 8 9
147818.6759	-5.4009	3	17.2578	17	305	8 0 8 7 8	7 0 7 7 8
166292.1826	-5.3691	3	22.1885	21	305	9 0 9 9 10	8 0 8 9 10
166292.9868	-3.5057	3	22.1885	19	305	9 0 9 8 9	8 0 8 7 8
166292.9935	-3.4616	3	22.1884	21	305	9 0 9 9 10	8 0 8 8 9
166292.9978	-3.4167	3	22.1885	23	305	9 0 9 10 11	8 0 8 9 10
166293.8999	-5.3652	3	22.1884	19	305	9 0 9 8 9	8 0 8 8 9
184766.7068	-5.3387	3	27.7354	23	305	10 0 10 10 11	9 0 9 10 11
184767.5168	-3.3794	3	27.7354	21	305	10 0 10 9 10	9 0 9 8 9
184767.5221	-3.3395	3	27.7354	23	305	10 0 10 10 11	9 0 9 9 10
184767.5256	-3.2989	3	27.7354	25	305	10 0 10 11 12	9 0 9 10 11
184768.4231	-5.3355	3	27.7354	21	305	10 0 10 9 10	9 0 9 9 10
203240.4516	-5.3135	3	33.8986	25	305	11 0 11 11 12	10 0 10 11 12
203241.2661	-3.2679	3	33.8986	23	305	11 0 11 10 11	10 0 10 9 10
203241.2704	-3.2313	3	33.8986	25	305	11 0 11 11 12	10 0 10 10 11
203241.2733	-3.1943	3	33.8986	27	305	11 0 11 12 13	10 0 10 11 12
203242.1671	-5.3108	3	33.8986	23	305	11 0 11 10 11	10 0 10 10 11

221713.3386	-5.2928	3	40.6780	27	305	12 0121213	11 0111213
221714.1568	-3.1686	3	40.6780	25	305	12 0121112	11 0111011
221714.1604	-3.1349	3	40.6779	27	305	12 0121213	11 0111112
221714.1629	-3.1009	3	40.6780	29	305	12 0121314	11 0111213
221715.0536	-5.2905	3	40.6779	25	305	12 0121112	11 0111112
240185.2898	-5.2762	3	48.0736	29	305	13 0131314	12 0121314
240186.1112	-3.0799	3	48.0736	27	305	13 0131213	12 0121112
240186.1141	-3.0486	3	48.0735	29	305	13 0131314	12 0121213
240186.1163	-3.0171	3	48.0736	31	305	13 0131415	12 0121314
240187.0044	-5.2741	3	48.0735	27	305	13 0131213	12 0121213
258656.2271	-5.2631	3	56.0853	31	305	14 0141415	13 0131415
258657.0511	-3.0003	3	56.0853	29	305	14 0141314	13 0131213
258657.0536	-2.9711	3	56.0853	31	305	14 0141415	13 0131314
258657.0555	-2.9708	3	56.0853	31	305	14 0141515	13 0131414
258657.9413	-5.2613	3	56.0853	29	305	14 0141314	13 0131314
277126.0723	-5.2824	3	64.7132	31	305	15 0151515	14 0141515
277126.8985	-2.9287	3	64.7132	31	305	15 0151415	14 0141314
277126.9007	-2.9305	3	64.7132	31	305	15 0151515	14 0141414
277126.9024	-2.9284	3	64.7132	31	305	15 0151615	14 0141514
277127.7862	-5.2518	3	64.7132	31	305	15 0151415	14 0141415
295594.7474	-5.2995	3	73.9571	31	305	16 0161615	15 0151615
295595.5756	-2.8933	3	73.9571	31	305	16 0161515	15 0151414
295595.5775	-2.8931	3	73.9571	31	305	16 0161615	15 0151514
295596.4611	-5.2743	3	73.9571	31	305	16 0161515	15 0151515
314063.0042	-2.8608	3	83.8172	31	305	17 0171615	16 0161514
314063.8878	-5.2944	3	83.8171	31	305	17 0171615	16 0161615

Table B4. Computed rotational transitions for gas phase CD_2CN^- by considering the experimental values of spectroscopic constants. Errors on the computed line frequencies are related to the errors on the constants given in Table 2 and from there, the error (dv/ν) on any line frequency for CD_2CN^- is found to be $= 3.77 \times 10^{-5}$.

Frequency (in MHz)	F^c	D^d	E_{lower}^e	g_{up}^f	QnF^h	Upper state (Qn_{up}^i)	Lower state (Qn_{lower}^j)
17491.5240	-6.7467	3	-0.0000	3	306	101121	000122
17491.5263	-6.8375	3	-0.0000	3	306	101111	000112
17491.5272	-6.2622	3	-0.0000	7	306	101233	000123
17491.5280	-6.3625	3	-0.0000	5	306	101222	000112
17491.5294	-6.7629	3	-0.0000	3	306	101211	000121
17491.5297	-6.5680	3	-0.0000	5	306	101122	000123
17491.5306	-6.9370	3	-0.0000	1	306	101110	000111
17492.2107	-6.4360	3	-0.0000	5	306	101112	000101
17492.2119	-6.2616	3	-0.0000	7	306	101123	000122
17492.2122	-6.7089	3	-0.0000	3	306	101101	000110
17492.2136	-6.0898	3	-0.0000	7	306	101223	000112
17492.2153	-5.9791	3	-0.0000	9	306	101234	000123
17492.2162	-6.3622	3	-0.0000	5	306	101212	000111
17492.2163	-6.7543	3	-0.0000	3	306	101011	000122
17492.2169	-6.4956	3	-0.0000	5	306	101012	000121
17493.2439	-6.5643	3	-0.0000	5	306	101232	000123
34983.4413	-6.8689	3	0.5835	5	306	202222	101011
34983.4415	-6.9289	3	0.5835	7	306	202233	101012
34983.4424	-6.9847	3	0.5835	3	306	202211	101212
34983.4430	-6.6835	3	0.5835	7	306	202233	101234
34983.4433	-6.8516	3	0.5835	3	306	202111	101010
34983.4434	-6.9706	3	0.5835	7	306	202333	101212
34983.4446	-6.9738	3	0.5835	3	306	202111	101012
34983.4450	-6.3605	3	0.5835	5	306	202122	101012
34983.4452	-6.3107	3	0.5835	5	306	202322	101212
34983.4455	-5.9790	3	0.5835	9	306	202344	101234
34983.4456	-6.8107	3	0.5835	5	306	202222	101123
34983.4460	-6.0650	3	0.5835	7	306	202333	101223
34983.4464	-6.5117	3	0.5835	3	306	202211	101101
34983.4465	-6.3150	3	0.5835	7	306	202233	101123
34983.4466	-6.8500	3	0.5835	1	306	202110	101011
34983.4468	-6.4550	3	0.5835	5	306	202222	101112
34983.4476	-6.8082	3	0.5835	7	306	202233	101112
34983.4478	-6.9684	3	0.5835	5	306	202322	101223
34983.4489	-6.6807	3	0.5835	9	306	202344	101123
34983.4492	-6.9814	3	0.5835	5	306	202322	101101
34983.4500	-6.9227	3	0.5835	5	306	202122	101123
34983.4507	-6.8627	3	0.5835	3	306	202111	101112
34983.5574	-6.5097	3	0.5835	1	306	202210	101221
34983.5582	-5.8121	3	0.5835	5	306	202232	101232
34983.5585	-6.2001	3	0.5835	3	306	202221	101210
34983.5600	-5.8118	3	0.5835	5	306	202332	101221
34983.5608	-5.6640	3	0.5835	7	306	202343	101232
34983.5617	-6.0355	3	0.5835	3	306	202321	101221
34983.5640	-6.1993	3	0.5835	3	306	202121	101232
34984.1278	-6.1593	3	0.5835	5	306	202222	101122
34984.1280	-6.1597	3	0.5835	3	306	202211	101110
34984.1281	-5.8786	3	0.5835	5	306	202222	101211
34984.1286	-5.7089	3	0.5835	7	306	202233	101122
34984.1312	-6.0114	3	0.5835	7	306	202233	101233
34984.1316	-5.5349	3	0.5835	7	306	202333	101222
34984.1317	-6.5110	3	0.5835	3	306	202111	101122

34984.1320	-6.5334	3	0.5835	3	306	202111	101211
34984.1322	-6.2869	3	0.5835	5	306	202122	101122
34984.1323	-6.2797	3	0.5835	3	306	202211	101111
34984.1325	-6.4787	3	0.5835	5	306	202122	101211
34984.1334	-6.2907	3	0.5835	5	306	202322	101222
34984.1337	-5.4253	3	0.5835	9	306	202344	101233
34984.1351	-5.8074	3	0.5835	5	306	202322	101111
34984.1375	-6.1897	3	0.5835	3	306	202111	101121
34984.1379	-5.9350	3	0.5835	5	306	202122	101121
34984.1389	-6.5467	3	0.5835	1	306	202110	101121
34984.1773	-6.3693	3	0.5835	5	306	202212	101212
34984.1777	-6.0879	3	0.5835	9	306	202234	101234
34984.1790	-6.1437	3	0.5835	7	306	202223	101123
34984.1797	-6.3216	3	0.5835	5	306	202112	101012
34984.1802	-5.5038	3	0.5835	7	306	202223	101112
34984.1803	-5.8073	3	0.5835	5	306	202112	101011
34984.1811	-5.3012	3	0.5835	9	306	202334	101223
34984.1813	-5.6317	3	0.5835	5	306	202212	101101
34984.1815	-5.4747	3	0.5835	7	306	202123	101012
34984.1818	-5.2125	3	0.5835	11	306	202345	101234
34984.1832	-6.1088	3	0.5835	3	306	202101	101010
34984.1843	-6.3696	3	0.5835	7	306	202323	101223
34984.1846	-6.9554	3	0.5835	5	306	202112	101123
34984.1858	-6.1983	3	0.5835	5	306	202112	101112
34984.1864	-6.3547	3	0.5835	7	306	202123	101123
34985.2727	-6.7772	3	0.5835	3	306	202221	101122
34985.2759	-6.0613	3	0.5835	5	306	202332	101222
34985.2776	-5.9668	3	0.5835	7	306	202343	101233
34985.2782	-6.4488	3	0.5835	3	306	202121	101122
34985.2784	-6.4764	3	0.5835	3	306	202221	101121
34985.2785	-6.4731	3	0.5835	3	306	202121	101211
34985.2793	-6.7612	3	0.5835	3	306	202321	101111
52475.2897	-6.8740	3	1.7504	7	306	303333	202112
52475.2909	-6.7947	3	1.7504	9	306	303344	202345
52475.2917	-6.8334	3	1.7504	5	306	303222	202101
52475.2932	-6.8544	3	1.7504	7	306	303333	202234
52475.2942	-6.5225	3	1.7504	3	306	303211	202101
52475.2943	-6.0668	3	1.7504	7	306	303233	202123
52475.2944	-6.0565	3	1.7504	7	306	303433	202323
52475.2945	-5.8318	3	1.7504	11	306	303455	202345
52475.2946	-6.4255	3	1.7504	5	306	303222	202112
52475.2948	-5.9056	3	1.7504	9	306	303444	202334
52475.2949	-6.1861	3	1.7504	5	306	303322	202212
52475.2950	-6.0282	3	1.7504	9	306	303344	202234
52475.2953	-6.1358	3	1.7504	7	306	303333	202223
52475.2971	-6.8305	3	1.7504	3	306	303211	202112
52475.2986	-6.7906	3	1.7504	11	306	303455	202234
52475.3002	-6.8678	3	1.7504	5	306	303222	202223
52475.9112	-6.6728	3	1.7504	5	306	303332	202343
52475.9121	-5.8568	3	1.7504	3	306	303321	202321
52475.9126	-5.5875	3	1.7504	7	306	303343	202343
52475.9135	-5.4538	3	1.7504	5	306	303332	202221
52475.9138	-5.7326	3	1.7504	5	306	303332	202232
52475.9143	-5.7640	3	1.7504	3	306	303221	202121
52475.9150	-5.5078	3	1.7504	5	306	303232	202121
52475.9152	-5.2813	3	1.7504	7	306	303343	202232
52475.9154	-5.1071	3	1.7504	7	306	303443	202332
52475.9163	-5.7303	3	1.7504	3	306	303321	202210

52475.9165	-4.9960	3	1.7504	9	306	3 0 3 4 5 4	2 0 2 3 4 3
52475.9166	-5.3780	3	1.7504	5	306	3 0 3 4 3 2	2 0 2 3 2 1
52475.9182	-6.8033	3	1.7504	5	306	3 0 3 2 3 2	2 0 2 3 4 3
52475.9183	-5.8589	3	1.7504	5	306	3 0 3 4 3 2	2 0 2 3 3 2
52475.9198	-6.0984	3	1.7504	3	306	3 0 3 2 2 1	2 0 2 2 2 1
52475.9201	-6.0766	3	1.7504	3	306	3 0 3 2 2 1	2 0 2 2 3 2
52475.9205	-6.0423	3	1.7504	5	306	3 0 3 2 3 2	2 0 2 2 2 1
52475.9208	-5.8523	3	1.7504	5	306	3 0 3 2 3 2	2 0 2 2 3 2
52475.9221	-6.4449	3	1.7504	1	306	3 0 3 2 1 0	2 0 2 2 2 1
52476.0270	-6.0354	3	1.7504	5	306	3 0 3 3 2 2	2 0 2 3 2 2
52476.0272	-5.7547	3	1.7504	9	306	3 0 3 3 4 4	2 0 2 3 4 4
52476.0278	-5.8141	3	1.7504	7	306	3 0 3 3 3 3	2 0 2 2 3 3
52476.0287	-5.1755	3	1.7504	7	306	3 0 3 3 3 3	2 0 2 2 2 2
52476.0292	-5.9885	3	1.7504	5	306	3 0 3 2 2 2	2 0 2 1 2 2
52476.0297	-5.0505	3	1.7504	9	306	3 0 3 3 4 4	2 0 2 2 3 3
52476.0299	-4.9731	3	1.7504	9	306	3 0 3 4 4 4	2 0 2 3 3 3
52476.0308	-4.8848	3	1.7504	11	306	3 0 3 4 5 5	2 0 2 3 4 4
52476.0309	-5.1337	3	1.7504	7	306	3 0 3 4 3 3	2 0 2 3 2 2
52476.0317	-6.9995	3	1.7504	3	306	3 0 3 2 1 1	2 0 2 1 2 2
52476.0322	-5.7826	3	1.7504	3	306	3 0 3 2 1 1	2 0 2 1 1 1
52476.0327	-6.0458	3	1.7504	7	306	3 0 3 4 3 3	2 0 2 3 3 3
52476.0331	-7.8450	3	1.7504	7	306	3 0 3 2 3 3	2 0 2 3 3 3
52476.0336	-5.8790	3	1.7504	5	306	3 0 3 2 2 2	2 0 2 2 2 2
52476.0343	-6.0331	3	1.7504	7	306	3 0 3 2 3 3	2 0 2 2 3 3
52476.0352	-6.8521	3	1.7504	7	306	3 0 3 2 3 3	2 0 2 2 2 2
52476.0361	-6.8754	3	1.7504	3	306	3 0 3 2 1 1	2 0 2 2 2 2
52476.0531	-6.1318	3	1.7504	7	306	3 0 3 3 2 3	2 0 2 3 2 3
52476.0534	-5.8470	3	1.7504	11	306	3 0 3 3 4 5	2 0 2 3 4 5
52476.0549	-5.8759	3	1.7504	9	306	3 0 3 3 3 4	2 0 2 2 3 4
52476.0551	-6.1056	3	1.7504	7	306	3 0 3 2 2 3	2 0 2 1 2 3
52476.0568	-5.1456	3	1.7504	7	306	3 0 3 2 2 3	2 0 2 1 1 2
52476.0570	-4.9745	3	1.7504	9	306	3 0 3 3 3 4	2 0 2 2 2 3
52476.0573	-4.8348	3	1.7504	11	306	3 0 3 4 4 5	2 0 2 3 3 4
52476.0575	-4.8784	3	1.7504	11	306	3 0 3 3 4 5	2 0 2 2 3 4
52476.0576	-4.9499	3	1.7504	9	306	3 0 3 4 3 4	2 0 2 3 2 3
52476.0577	-4.7609	3	1.7504	13	306	3 0 3 4 5 6	2 0 2 3 4 5
52476.0602	-5.8480	3	1.7504	5	306	3 0 3 2 1 2	2 0 2 1 1 2
52476.0603	-6.9782	3	1.7504	7	306	3 0 3 2 2 3	2 0 2 2 3 4
52476.0608	-6.1342	3	1.7504	9	306	3 0 3 4 3 4	2 0 2 3 3 4
52476.0625	-5.8938	3	1.7504	7	306	3 0 3 2 2 3	2 0 2 2 2 3
52476.0628	-6.1217	3	1.7504	9	306	3 0 3 2 3 4	2 0 2 2 3 4
52477.0545	-6.6825	3	1.7504	5	306	3 0 3 3 3 2	2 0 2 1 1 1
52477.0554	-6.7445	3	1.7504	7	306	3 0 3 3 4 3	2 0 2 1 2 2
52477.0562	-6.8136	3	1.7504	3	306	3 0 3 3 2 1	2 0 2 3 2 2
52477.0565	-6.5100	3	1.7504	7	306	3 0 3 3 4 3	2 0 2 3 4 4
52477.0576	-6.6271	3	1.7504	5	306	3 0 3 3 3 2	2 0 2 2 3 3
52477.0579	-6.7952	3	1.7504	7	306	3 0 3 4 4 3	2 0 2 3 2 2
52477.0584	-6.2707	3	1.7504	5	306	3 0 3 3 3 2	2 0 2 2 2 2
52477.0589	-6.1326	3	1.7504	7	306	3 0 3 3 4 3	2 0 2 2 3 3
52477.0591	-6.3296	3	1.7504	3	306	3 0 3 3 2 1	2 0 2 2 1 1
52477.0594	-6.6884	3	1.7504	3	306	3 0 3 2 2 1	2 0 2 1 1 0
52477.0597	-5.8903	3	1.7504	7	306	3 0 3 4 4 3	2 0 2 3 3 3
52477.0598	-6.6287	3	1.7504	7	306	3 0 3 3 4 3	2 0 2 2 2 2
52477.0603	-6.8110	3	1.7504	3	306	3 0 3 2 2 1	2 0 2 1 2 2
52477.0604	-5.8094	3	1.7504	9	306	3 0 3 4 5 4	2 0 2 3 4 4
52477.0608	-6.1447	3	1.7504	5	306	3 0 3 4 3 2	2 0 2 3 2 2
52477.0611	-6.1988	3	1.7504	5	306	3 0 3 2 3 2	2 0 2 1 2 2
52477.0615	-6.8125	3	1.7504	5	306	3 0 3 2 3 2	2 0 2 1 1 1

52477.0626	-6.7966	3	1.7504	5	306	3 0 3 4 3 2	2 0 2 3 3 3
52477.0629	-6.5118	3	1.7504	9	306	3 0 3 4 5 4	2 0 2 2 3 3
52477.0631	-6.6895	3	1.7504	1	306	3 0 3 2 1 0	2 0 2 1 1 1
52477.0636	-6.8158	3	1.7504	5	306	3 0 3 4 3 2	2 0 2 2 1 1
52477.0646	-6.7484	3	1.7504	5	306	3 0 3 2 3 2	2 0 2 2 3 3
52477.0647	-6.6863	3	1.7504	3	306	3 0 3 2 2 1	2 0 2 2 2 2
69966.9584	-6.9358	3	3.5008	9	306	4 0 4 4 4 4	3 0 3 2 2 3
69966.9594	-6.8910	3	3.5008	11	306	4 0 4 4 5 5	3 0 3 4 5 6
69966.9601	-6.9064	3	3.5008	7	306	4 0 4 3 3 3	3 0 3 2 1 2
69966.9613	-6.9265	3	3.5008	9	306	4 0 4 4 4 4	3 0 3 3 4 5
69966.9632	-6.1942	3	3.5008	5	306	4 0 4 3 2 2	3 0 3 2 1 2
69966.9633	-5.9056	3	3.5008	9	306	4 0 4 5 4 4	3 0 3 4 3 4
69966.9634	-5.7321	3	3.5008	13	306	4 0 4 5 6 6	3 0 3 4 5 6
69966.9635	-6.1214	3	3.5008	7	306	4 0 4 3 3 3	3 0 3 2 2 3
69966.9636	-5.7965	3	3.5008	11	306	4 0 4 5 5 5	3 0 3 4 4 5
69966.9637	-5.8696	3	3.5008	11	306	4 0 4 4 5 5	3 0 3 3 4 5
69966.9639	-5.9550	3	3.5008	9	306	4 0 4 4 4 4	3 0 3 3 3 4
69966.9663	-6.9234	3	3.5008	11	306	4 0 4 4 5 5	3 0 3 3 3 4
69966.9666	-6.9029	3	3.5008	5	306	4 0 4 3 2 2	3 0 3 2 2 3
69966.9677	-6.8866	3	3.5008	13	306	4 0 4 5 6 6	3 0 3 3 4 5
69966.9689	-6.9298	3	3.5008	7	306	4 0 4 3 3 3	3 0 3 3 3 4
69967.6711	-6.8581	3	3.5008	7	306	4 0 4 4 4 3	3 0 3 4 5 4
69967.6729	-5.7640	3	3.5008	5	306	4 0 4 4 3 2	3 0 3 4 3 2
69967.6733	-5.4827	3	3.5008	9	306	4 0 4 4 5 4	3 0 3 4 5 4
69967.6751	-5.5401	3	3.5008	7	306	4 0 4 4 4 3	3 0 3 3 4 3
69967.6753	-5.7159	3	3.5008	5	306	4 0 4 3 3 2	3 0 3 2 3 2
69967.6760	-5.2029	3	3.5008	5	306	4 0 4 3 3 2	3 0 3 2 2 1
69967.6764	-4.9008	3	3.5008	7	306	4 0 4 4 4 3	3 0 3 3 3 2
69967.6767	-5.5042	3	3.5008	3	306	4 0 4 3 2 1	3 0 3 2 1 0
69967.6770	-4.6977	3	3.5008	9	306	4 0 4 5 5 4	3 0 3 4 4 3
69967.6771	-4.8706	3	3.5008	7	306	4 0 4 3 4 3	3 0 3 2 3 2
69967.6773	-4.7748	3	3.5008	9	306	4 0 4 4 5 4	3 0 3 3 4 3
69967.6775	-4.8578	3	3.5008	7	306	4 0 4 5 4 3	3 0 3 4 3 2
69967.6776	-4.6089	3	3.5008	11	306	4 0 4 5 6 5	3 0 3 4 5 4
69967.6783	-6.7246	3	3.5008	3	306	4 0 4 3 2 1	3 0 3 2 3 2
69967.6790	-5.5053	3	3.5008	3	306	4 0 4 3 2 1	3 0 3 2 2 1
69967.6804	-5.7673	3	3.5008	7	306	4 0 4 5 4 3	3 0 3 4 4 3
69967.6809	-6.3543	3	3.5008	5	306	4 0 4 3 3 2	3 0 3 3 4 3
69967.6822	-5.5977	3	3.5008	5	306	4 0 4 3 3 2	3 0 3 3 3 2
69967.6828	-5.7529	3	3.5008	7	306	4 0 4 3 4 3	3 0 3 3 4 3
69967.6841	-6.5733	3	3.5008	7	306	4 0 4 3 4 3	3 0 3 3 3 2
69967.6853	-6.5911	3	3.5008	3	306	4 0 4 3 2 1	3 0 3 3 3 2
69967.7224	-5.8942	3	3.5008	7	306	4 0 4 4 3 3	3 0 3 4 3 3
69967.7226	-5.6097	3	3.5008	11	306	4 0 4 4 5 5	3 0 3 4 5 5
69967.7238	-5.6407	3	3.5008	9	306	4 0 4 4 4 4	3 0 3 3 4 4
69967.7242	-5.8687	3	3.5008	7	306	4 0 4 3 3 3	3 0 3 2 3 3
69967.7256	-4.7411	3	3.5008	9	306	4 0 4 4 4 4	3 0 3 3 3 3
69967.7258	-4.9116	3	3.5008	7	306	4 0 4 3 3 3	3 0 3 2 2 2
69967.7261	-4.6014	3	3.5008	11	306	4 0 4 5 5 5	3 0 3 4 4 4
69967.7262	-4.6453	3	3.5008	11	306	4 0 4 4 5 5	3 0 3 3 4 4
69967.7263	-5.0550	3	3.5008	5	306	4 0 4 3 2 2	3 0 3 2 1 1
69967.7264	-4.7198	3	3.5008	9	306	4 0 4 3 4 4	3 0 3 2 3 3
69967.7265	-4.7165	3	3.5008	9	306	4 0 4 5 4 4	3 0 3 4 3 3
69967.7266	-4.5276	3	3.5008	13	306	4 0 4 5 6 6	3 0 3 4 5 5
69967.7288	-6.7481	3	3.5008	7	306	4 0 4 3 3 3	3 0 3 3 4 4
69967.7289	-5.6171	3	3.5008	5	306	4 0 4 3 2 2	3 0 3 2 2 2
69967.7294	-5.9040	3	3.5008	9	306	4 0 4 5 4 4	3 0 3 4 4 4
69967.7307	-5.6661	3	3.5008	7	306	4 0 4 3 3 3	3 0 3 3 3 3

69967.7311	-5.8927	3	3.5008	9	306	4 0 4 3 4 4	3 0 3 3 4 4
69967.7337	-6.9988	3	3.5008	5	306	4 0 4 3 2 2	3 0 3 3 3 3
69967.7391	-5.9785	3	3.5008	9	306	4 0 4 4 3 4	3 0 3 4 3 4
69967.7394	-5.6936	3	3.5008	13	306	4 0 4 4 5 6	3 0 3 4 5 6
69967.7407	-5.7101	3	3.5008	11	306	4 0 4 4 4 5	3 0 3 3 4 5
69967.7408	-5.9612	3	3.5008	9	306	4 0 4 3 3 4	3 0 3 2 3 4
69967.7432	-4.7265	3	3.5008	9	306	4 0 4 3 3 4	3 0 3 2 2 3
69967.7434	-4.6066	3	3.5008	11	306	4 0 4 4 4 5	3 0 3 3 3 4
69967.7435	-4.5008	3	3.5008	13	306	4 0 4 5 5 6	3 0 3 4 4 5
69967.7436	-4.5920	3	3.5008	11	306	4 0 4 3 4 5	3 0 3 2 3 4
69967.7437	-4.5288	3	3.5008	13	306	4 0 4 4 5 6	3 0 3 3 4 5
69967.7438	-4.4373	3	3.5008	15	306	4 0 4 5 6 7	3 0 3 4 5 6
69967.7468	-5.6879	3	3.5008	7	306	4 0 4 3 2 3	3 0 3 2 2 3
69967.7472	-5.9818	3	3.5008	11	306	4 0 4 5 4 5	3 0 3 4 4 5
69967.7487	-5.7179	3	3.5008	9	306	4 0 4 3 3 4	3 0 3 3 3 4
69967.7489	-5.9715	3	3.5008	11	306	4 0 4 3 4 5	3 0 3 3 4 5
69968.7013	-6.7383	3	3.5008	7	306	4 0 4 4 4 3	3 0 3 2 2 2
69968.7019	-6.9334	3	3.5008	9	306	4 0 4 4 5 4	3 0 3 2 3 3
69968.7027	-6.9720	3	3.5008	5	306	4 0 4 4 3 2	3 0 3 4 3 3
69968.7029	-6.6739	3	3.5008	9	306	4 0 4 4 5 4	3 0 3 4 5 5
69968.7040	-6.9621	3	3.5008	9	306	4 0 4 5 5 4	3 0 3 4 3 3
69968.7043	-6.7265	3	3.5008	7	306	4 0 4 4 4 3	3 0 3 3 4 4
69968.7046	-6.7130	3	3.5008	5	306	4 0 4 3 3 2	3 0 3 2 1 1
69968.7055	-6.9595	3	3.5008	5	306	4 0 4 3 3 2	3 0 3 2 3 3
69968.7062	-6.0061	3	3.5008	7	306	4 0 4 4 4 3	3 0 3 3 3 3
69968.7065	-5.9018	3	3.5008	9	306	4 0 4 4 5 4	3 0 3 3 4 4
69968.7066	-6.0607	3	3.5008	5	306	4 0 4 4 3 2	3 0 3 3 2 2
69968.7068	-5.7835	3	3.5008	9	306	4 0 4 5 5 4	3 0 3 4 4 4
69968.7071	-6.3093	3	3.5008	5	306	4 0 4 3 3 2	3 0 3 2 2 2
69968.7072	-5.7140	3	3.5008	11	306	4 0 4 5 6 5	3 0 3 4 5 5
69968.7073	-5.9408	3	3.5008	7	306	4 0 4 5 4 3	3 0 3 4 3 3
69968.7074	-5.9524	3	3.5008	7	306	4 0 4 3 4 3	3 0 3 2 3 3
69968.7076	-6.4112	3	3.5008	3	306	4 0 4 3 2 1	3 0 3 2 1 1
69968.7084	-6.7286	3	3.5008	9	306	4 0 4 4 5 4	3 0 3 3 3 3
69968.7090	-6.9616	3	3.5008	7	306	4 0 4 3 4 3	3 0 3 2 2 2
69968.7101	-6.7152	3	3.5008	3	306	4 0 4 3 2 1	3 0 3 2 2 2
69968.7102	-6.9645	3	3.5008	7	306	4 0 4 5 4 3	3 0 3 4 4 4
69968.7108	-6.6769	3	3.5008	11	306	4 0 4 5 6 6	3 0 3 3 4 4
69968.7112	-6.9753	3	3.5008	7	306	4 0 4 5 4 3	3 0 3 3 2 2
69968.7120	-6.7429	3	3.5008	5	306	4 0 4 3 3 2	3 0 3 3 3 3
87458.3688	-6.9756	3	5.8347	13	306	5 0 5 5 6 6	4 0 4 5 6 7
87458.3695	-6.9829	3	5.8347	9	306	5 0 5 4 4 4	4 0 4 3 2 3
87458.3704	-6.9996	3	5.8347	11	306	5 0 5 5 5 5	4 0 4 4 5 6
87458.3729	-5.7995	3	5.8347	11	306	5 0 5 6 5 5	4 0 4 5 4 5
87458.3730	-5.6571	3	5.8347	15	306	5 0 5 6 7 7	4 0 4 5 6 7
87458.3731	-5.7140	3	5.8347	13	306	5 0 5 6 6 6	4 0 4 5 5 6
87458.3732	-5.7623	3	5.8347	13	306	5 0 5 5 6 6	4 0 4 4 5 6
87458.3733	-5.8335	3	5.8347	11	306	5 0 5 5 5 5	4 0 4 4 4 5
87458.3761	-6.9962	3	5.8347	13	306	5 0 5 5 6 6	4 0 4 4 4 5
87458.3765	-6.9791	3	5.8347	7	306	5 0 5 4 3 3	4 0 4 3 3 4
87458.3774	-6.9711	3	5.8347	15	306	5 0 5 6 7 7	4 0 4 4 5 6
87458.3784	-6.9988	3	5.8347	9	306	5 0 5 4 4 4	4 0 4 4 4 5
87459.1214	-5.6933	3	5.8347	7	306	5 0 5 5 4 3	4 0 4 5 4 3
87459.1217	-5.4085	3	5.8347	11	306	5 0 5 5 6 5	4 0 4 5 6 5
87459.1233	-6.9650	3	5.8347	11	306	5 0 5 6 6 5	4 0 4 5 6 5
87459.1234	-5.4381	3	5.8347	9	306	5 0 5 5 5 4	4 0 4 4 5 4
87459.1253	-4.7079	3	5.8347	7	306	5 0 5 4 4 3	4 0 4 3 3 2
87459.1256	-4.5372	3	5.8347	9	306	5 0 5 5 5 4	4 0 4 4 4 3

87459.1258	-4.3973	3	5.8347	11	306	5 0 5 6 6 5	4 0 4 5 5 4
87459.1259	-4.5156	3	5.8347	9	306	5 0 5 4 5 4	4 0 4 3 4 3
87459.1260	-4.4411	3	5.8347	11	306	5 0 5 5 6 5	4 0 4 4 5 4
87459.1262	-4.3233	3	5.8347	13	306	5 0 5 6 7 6	4 0 4 5 6 5
87459.1287	-5.4109	3	5.8347	5	306	5 0 5 4 3 2	4 0 4 3 3 2
87459.1289	-6.5420	3	5.8347	7	306	5 0 5 4 4 3	4 0 4 4 5 4
87459.1294	-5.6974	3	5.8347	9	306	5 0 5 6 5 4	4 0 4 5 5 4
87459.1311	-5.4577	3	5.8347	7	306	5 0 5 4 4 3	4 0 4 4 4 3
87459.1314	-5.6851	3	5.8347	9	306	5 0 5 4 5 4	4 0 4 4 5 4
87459.1336	-6.8842	3	5.8347	9	306	5 0 5 4 5 5	4 0 4 4 4 3
87459.1345	-6.7880	3	5.8347	5	306	5 0 5 4 3 2	4 0 4 4 4 3
87459.1490	-5.7949	3	5.8347	9	306	5 0 5 5 4 4	4 0 4 5 4 4
87459.1492	-5.5101	3	5.8347	13	306	5 0 5 5 6 6	4 0 4 5 6 6
87459.1504	-5.5280	3	5.8347	11	306	5 0 5 5 5 5	4 0 4 4 5 5
87459.1505	-6.9159	3	5.8347	13	306	5 0 5 6 6 6	4 0 4 5 6 6
87459.1506	-5.7781	3	5.8347	9	306	5 0 5 4 4 4	4 0 4 3 4 4
87459.1528	-4.4262	3	5.8347	11	306	5 0 5 5 5 5	4 0 4 4 4 4
87459.1531	-4.3204	3	5.8347	13	306	5 0 5 6 6 6	4 0 4 5 5 5
87459.1532	-4.3485	3	5.8347	13	306	5 0 5 5 6 6	4 0 4 4 5 5
87459.1533	-4.4103	3	5.8347	11	306	5 0 5 6 5 5	4 0 4 5 4 4
87459.1534	-4.2570	3	5.8347	15	306	5 0 5 6 7 7	4 0 4 5 6 6
87459.1555	-6.8478	3	5.8347	9	306	5 0 5 4 4 4	4 0 4 4 5 5
87459.1562	-5.5097	3	5.8347	7	306	5 0 5 4 3 3	4 0 4 3 3 3
87459.1566	-5.8040	3	5.8347	11	306	5 0 5 6 5 5	4 0 4 5 5 5
87459.1579	-5.5416	3	5.8347	9	306	5 0 5 4 4 4	4 0 4 4 4 4
87459.1581	-5.7944	3	5.8347	11	306	5 0 5 4 5 5	4 0 4 4 5 5
87459.1607	-5.8677	3	5.8347	11	306	5 0 5 5 4 5	4 0 4 5 4 5
87459.1608	-5.5847	3	5.8347	15	306	5 0 5 5 6 7	4 0 4 5 6 7
87459.1620	-6.8626	3	5.8347	15	306	5 0 5 6 6 7	4 0 4 5 6 7
87459.1621	-5.5944	3	5.8347	13	306	5 0 5 5 5 6	4 0 4 4 5 6
87459.1649	-4.4179	3	5.8347	11	306	5 0 5 4 4 5	4 0 4 3 3 4
87459.1650	-4.3254	3	5.8347	13	306	5 0 5 5 5 6	4 0 4 4 4 5
87459.1651	-4.2405	3	5.8347	15	306	5 0 5 6 6 7	4 0 4 5 5 6
87459.1652	-4.2598	3	5.8347	15	306	5 0 5 5 6 7	4 0 4 4 5 6
87459.1653	-4.1848	3	5.8347	17	306	5 0 5 6 7 8	4 0 4 5 6 7
87459.1686	-5.5757	3	5.8347	9	306	5 0 5 4 3 4	4 0 4 3 3 4
87459.1689	-5.8712	3	5.8347	13	306	5 0 5 6 5 6	4 0 4 5 5 6
87459.1702	-5.5982	3	5.8347	11	306	5 0 5 4 4 5	4 0 4 4 4 5
87459.1704	-5.8625	3	5.8347	13	306	5 0 5 4 5 6	4 0 4 4 5 6
87460.1011	-6.8299	3	5.8347	9	306	5 0 5 5 5 4	4 0 4 3 3 3
87460.1024	-6.7996	3	5.8347	11	306	5 0 5 5 6 5	4 0 4 5 6 6
87460.1036	-6.8118	3	5.8347	7	306	5 0 5 4 4 3	4 0 4 3 2 2
87460.1037	-6.8295	3	5.8347	9	306	5 0 5 5 5 4	4 0 4 4 5 5
87460.1061	-5.8563	3	5.8347	9	306	5 0 5 5 5 4	4 0 4 4 4 4
87460.1064	-5.7741	3	5.8347	11	306	5 0 5 5 6 5	4 0 4 4 5 5
87460.1065	-5.7038	3	5.8347	11	306	5 0 5 6 6 5	4 0 4 5 5 5
87460.1066	-6.0316	3	5.8347	7	306	5 0 5 4 4 3	4 0 4 3 3 3
87460.1068	-5.6432	3	5.8347	13	306	5 0 5 6 7 6	4 0 4 5 6 6
87460.1069	-5.8221	3	5.8347	9	306	5 0 5 4 5 4	4 0 4 3 4 4
87460.1088	-6.8320	3	5.8347	11	306	5 0 5 5 6 5	4 0 4 4 4 4
87460.1100	-6.8146	3	5.8347	5	306	5 0 5 4 3 2	4 0 4 3 3 3
87460.1108	-6.8031	3	5.8347	13	306	5 0 5 6 7 6	4 0 4 4 5 5
87460.1117	-6.8346	3	5.8347	7	306	5 0 5 4 4 3	4 0 4 4 4 4
104949.4514	-5.7188	3	8.7520	13	306	6 0 6 7 6 6	5 0 5 6 5 6
104949.4515	-5.5976	3	8.7520	17	306	6 0 6 7 8 8	5 0 5 6 7 8
104949.4516	-5.6485	3	8.7520	15	306	6 0 6 7 7 7	5 0 5 6 6 7
104949.4517	-5.7437	3	8.7520	13	306	6 0 6 6 6 6	5 0 5 5 5 6
104950.2218	-5.6361	3	8.7520	9	306	6 0 6 6 5 4	5 0 5 6 5 4

104950.2219	-6.8899	3	8.7520	11	306	606665	505665
104950.2220	-5.3512	3	8.7520	13	306	606676	505676
104950.2233	-6.7545	3	8.7520	13	306	606776	505676
104950.2234	-5.3681	3	8.7520	11	306	606665	505565
104950.2259	-4.3846	3	8.7520	9	306	606554	505443
104950.2261	-4.2649	3	8.7520	11	306	606665	505554
104950.2262	-4.1590	3	8.7520	13	306	606776	505665
104950.2263	-4.2488	3	8.7520	11	306	606765	505654
104950.2264	-4.0954	3	8.7520	15	306	606787	505676
104950.2265	-6.8870	3	8.7520	11	306	606565	505654
104950.2288	-6.6851	3	8.7520	9	306	606554	505565
104950.2295	-5.3464	3	8.7520	7	306	606543	505443
104950.2299	-5.6404	3	8.7520	11	306	606765	505665
104950.2315	-5.3769	3	8.7520	9	306	606554	505554
104950.2316	-5.6302	3	8.7520	11	306	606565	505565
104950.2350	-6.9407	3	8.7520	7	306	606543	505554
104950.2393	-5.7190	3	8.7520	11	306	606655	505655
104950.2393	-6.8264	3	8.7520	13	306	606666	505666
104950.2395	-5.4361	3	8.7520	15	306	606677	505677
104950.2406	-5.4467	3	8.7520	13	306	606666	505566
104950.2407	-5.7066	3	8.7520	11	306	606555	505455
104950.2434	-4.1793	3	8.7520	13	306	606666	505555
104950.2435	-6.9313	3	8.7520	13	306	606766	505455
104950.2436	-4.0944	3	8.7520	15	306	606777	505666
104950.2437	-4.1138	3	8.7520	15	306	606677	505566
104950.2438	-4.0388	3	8.7520	17	306	606788	505677
104950.2457	-6.9357	3	8.7520	11	306	606555	505566
104950.2469	-5.4316	3	8.7520	9	306	606544	505444
104950.2469	-6.8276	3	8.7520	11	306	606655	505555
104950.2472	-5.7273	3	8.7520	13	306	606766	505666
104950.2479	-5.7824	3	8.7520	13	306	606656	505656
104950.2480	-5.5027	3	8.7520	17	306	606678	505678
104950.2484	-5.4554	3	8.7520	11	306	606555	505555
104950.2486	-5.7191	3	8.7520	13	306	606566	505566
104950.2488	-6.9878	3	8.7520	9	306	606544	505544
104950.2491	-6.6759	3	8.7520	17	306	606778	505678
104950.2492	-5.5082	3	8.7520	15	306	606667	505567
104950.2522	-4.1741	3	8.7520	13	306	606556	505445
104950.2523	-4.0986	3	8.7520	15	306	606667	505556
104950.2524	-4.0277	3	8.7520	17	306	606778	505667
104950.2525	-3.9782	3	8.7520	19	306	606789	505678
104950.2526	-6.9742	3	8.7520	15	306	606567	505656
104950.2560	-5.4918	3	8.7520	11	306	606545	505445
104950.2562	-5.7858	3	8.7520	15	306	606767	505667
104950.2575	-5.5102	3	8.7520	13	306	606556	505556
104950.2576	-6.8964	3	8.7520	11	306	606545	505545
104951.1744	-6.9182	3	8.7520	11	306	606665	505444
104951.1754	-6.9033	3	8.7520	13	306	606676	505677
104951.1763	-6.9057	3	8.7520	9	306	606554	505433
104951.1766	-6.9226	3	8.7520	11	306	606665	505564
104951.1794	-5.7549	3	8.7520	11	306	606665	505555
104951.1796	-5.6868	3	8.7520	13	306	606676	505566
104951.1797	-5.6404	3	8.7520	13	306	606776	505666
104951.1798	-5.5869	3	8.7520	15	306	606787	505677
104951.1799	-5.7301	3	8.7520	11	306	606765	505655
104951.1824	-6.9254	3	8.7520	13	306	606676	505555
104951.1833	-6.9088	3	8.7520	7	306	606543	505444
104951.1840	-6.9071	3	8.7520	15	306	606787	505566

104951.1848	-6.9230	3	8.7520	9	306	606554	505555
122440.1294	-5.5489	3	12.2528	19	306	707899	606789
122440.1295	-5.5950	3	12.2528	17	306	707888	606778
122440.1296	-5.6739	3	12.2528	15	306	707777	606667
122440.9138	-5.5886	3	12.2528	11	306	707765	606765
122440.9139	-6.6942	3	12.2528	13	306	707776	606776
122440.9140	-5.3056	3	12.2528	15	306	707787	606787
122440.9152	-6.5838	3	12.2528	15	306	707887	606787
122440.9153	-5.3155	3	12.2528	13	306	707776	606676
122440.9171	-6.8974	3	12.2528	15	306	707787	606776
122440.9181	-4.1392	3	12.2528	11	306	707665	606554
122440.9182	-4.0468	3	12.2528	13	306	707776	606665
122440.9183	-3.9618	3	12.2528	15	306	707887	606776
122440.9184	-3.9811	3	12.2528	15	306	707787	606674
122440.9185	-3.9061	3	12.2528	17	306	707898	606787
122440.9200	-6.9837	3	12.2528	11	306	707665	606654
122440.9205	-6.8022	3	12.2528	11	306	707665	606676
122440.9218	-5.2973	3	12.2528	9	306	707654	606554
122440.9221	-5.5929	3	12.2528	13	306	707876	606776
122440.9235	-5.3200	3	12.2528	11	306	707665	606665
122440.9236	-5.5842	3	12.2528	13	306	707676	606676
122440.9237	-6.8550	3	12.2528	9	306	707654	606654
122440.9260	-5.6583	3	12.2528	13	306	707766	606766
122440.9261	-5.3787	3	12.2528	17	306	707788	606788
122440.9272	-5.3849	3	12.2528	15	306	707777	606677
122440.9292	-6.9030	3	12.2528	17	306	707788	606777
122440.9302	-3.9768	3	12.2528	15	306	707777	606666
122440.9303	-3.9059	3	12.2528	17	306	707888	606777
122440.9304	-3.8564	3	12.2528	19	306	707899	606788
122440.9305	-6.8526	3	12.2528	15	306	707677	606766
122440.9317	-6.9691	3	12.2528	13	306	707666	606655
122440.9326	-5.4388	3	12.2528	19	306	707789	606789
122440.9337	-5.4416	3	12.2528	17	306	707778	606678
122440.9338	-6.6463	3	12.2528	13	306	707766	606666
122440.9339	-5.3717	3	12.2528	11	306	707655	606555
122440.9340	-5.6658	3	12.2528	15	306	707877	606777
122440.9352	-5.3910	3	12.2528	13	306	707666	606666
122440.9353	-5.6586	3	12.2528	15	306	707677	606677
122440.9354	-6.7748	3	12.2528	11	306	707655	606655
122440.9360	-6.9090	3	12.2528	19	306	707789	606778
122440.9369	-3.9731	3	12.2528	15	306	707667	606556
122440.9370	-3.8486	3	12.2528	19	306	707889	606778
122440.9371	-3.8040	3	12.2528	21	306	7078910	606789
122440.9372	-6.9103	3	12.2528	17	306	707678	606767
122440.9384	-6.9562	3	12.2528	15	306	707667	606656
122440.9408	-5.4267	3	12.2528	13	306	707656	606556
122440.9409	-5.7173	3	12.2528	17	306	707878	606778
122440.9421	-5.4426	3	12.2528	15	306	707667	606667
122440.9422	-6.7060	3	12.2528	13	306	707656	606656
122441.8501	-6.9930	3	12.2528	15	306	707787	606788
122441.8509	-6.9906	3	12.2528	11	306	707665	606544
122441.8542	-5.6795	3	12.2528	13	306	707776	606666
122441.8544	-5.5885	3	12.2528	15	306	707887	606777
122441.8545	-5.5405	3	12.2528	17	306	707898	606788
122441.8546	-5.6624	3	12.2528	13	306	707876	606766
122441.8581	-6.9939	3	12.2528	9	306	707654	606555
122441.8588	-6.9969	3	12.2528	17	306	707898	606677
139930.3385	-5.5506	3	16.3370	19	306	808999	707889

139931.1327	-5.5486	3	16.3370	13	306	808876	707876
139931.1328	-5.2689	3	16.3370	17	306	808898	707898
139931.1340	-5.2745	3	16.3370	15	306	808887	707787
139931.1361	-6.7920	3	16.3370	17	306	808898	707887
139931.1371	-3.9406	3	16.3370	13	306	808776	707665
139931.1372	-3.7943	3	16.3370	17	306	808998	707887
139931.1373	-3.7447	3	16.3370	19	306	8089109	707898
139931.1374	-6.7407	3	16.3370	15	306	808787	707876
139931.1387	-6.8565	3	16.3370	13	306	808776	707765
139931.1392	-6.9027	3	16.3370	13	306	808776	707787
139931.1409	-5.2585	3	16.3370	11	306	808765	707665
139931.1411	-5.5525	3	16.3370	15	306	808987	707887
139931.1416	-5.6085	3	16.3370	15	306	808877	707877
139931.1417	-5.3332	3	16.3370	19	306	808899	707899
139931.1423	-5.2770	3	16.3370	13	306	808776	707776
139931.1424	-5.5450	3	16.3370	15	306	808787	707787
139931.1425	-6.6629	3	16.3370	11	306	808765	707765
139931.1427	-6.4189	3	16.3370	19	306	808999	707899
139931.1428	-5.3366	3	16.3370	17	306	808888	707788
139931.1450	-6.8044	3	16.3370	19	306	808899	707888
139931.1459	-3.8694	3	16.3370	15	306	808777	707667
139931.1460	-3.7449	3	16.3370	19	306	808999	707888
139931.1461	-3.7003	3	16.3370	21	306	80891010	707899
139931.1462	-6.8069	3	16.3370	17	306	808788	707877
139931.1468	-5.6582	3	16.3370	17	306	808878	707878
139931.1469	-5.3881	3	16.3370	21	306	8088910	7078910
139931.1473	-6.8537	3	16.3370	15	306	808777	707766
139931.1479	-5.3889	3	16.3370	19	306	808889	707789
139931.1497	-5.3247	3	16.3370	13	306	808766	707666
139931.1498	-5.6152	3	16.3370	17	306	808988	707888
139931.1504	-6.8180	3	16.3370	21	306	8088910	707889
139931.1509	-5.3412	3	16.3370	15	306	808777	707777
139931.1510	-5.6088	3	16.3370	17	306	808788	707788
139931.1511	-6.6027	3	16.3370	13	306	808766	707766
139931.1513	-3.7476	3	16.3370	19	306	808889	707778
139931.1513	-3.6945	3	16.3370	21	306	8089910	707889
139931.1514	-3.6540	3	16.3370	23	306	80891011	7078910
139931.1515	-6.8715	3	16.3370	19	306	808789	707878
139931.1526	-6.8519	3	16.3370	17	306	808778	707767
139931.1551	-5.3752	3	16.3370	15	306	808767	707667
139931.1552	-6.4610	3	16.3370	17	306	808878	707778
139931.1553	-5.6610	3	16.3370	19	306	808989	707889
139931.1563	-5.3894	3	16.3370	17	306	808778	707778
139931.1564	-5.6549	3	16.3370	19	306	808789	707789
139932.0612	-5.6204	3	16.3370	15	306	808887	707777
139932.0613	-5.5452	3	16.3370	17	306	808998	707888
139932.0614	-5.6081	3	16.3370	15	306	808987	707877
139932.0614	-5.5018	3	16.3370	19	306	8089109	707899
139932.0615	-5.7487	3	16.3370	11	306	808765	707655
157420.0105	-5.4748	3	21.0046	23	306	909101111	80891011
157420.0106	-5.5284	3	21.0046	21	306	90991010	8088910
157420.8122	-5.5146	3	21.0046	15	306	909987	808987
157420.8123	-5.2393	3	21.0046	19	306	9099109	8089109
157420.8133	-6.3235	3	21.0046	19	306	90910109	8089109
157420.8134	-5.2422	3	21.0046	17	306	909998	808898
157420.8157	-6.7095	3	21.0046	19	306	9099109	808998
157420.8166	-3.7739	3	21.0046	15	306	909887	808776
157420.8167	-3.6493	3	21.0046	19	306	90910109	808998

157420.8168	-3.6047	3	21.0046	21	306	9 0 9 10 11 10	8 0 8 9 10 9
157420.8178	-6.9489	3	21.0046	19	306	9 0 9 10 10 9	8 0 8 8 9 8
157420.8180	-6.7572	3	21.0046	15	306	9 0 9 8 8 7	8 0 8 8 7 6
157420.8184	-6.9920	3	21.0046	15	306	9 0 9 8 8 7	8 0 8 8 9 8
157420.8190	-5.5670	3	21.0046	17	306	9 0 9 9 8 8	8 0 8 9 8 8
157420.8191	-5.2969	3	21.0046	21	306	9 0 9 9 10 10	8 0 8 9 10 10
157420.8200	-6.3052	3	21.0046	21	306	9 0 9 10 10 10	8 0 8 9 10 10
157420.8201	-5.2983	3	21.0046	19	306	9 0 9 9 9 9	8 0 8 8 9 9
157420.8204	-5.2276	3	21.0046	13	306	9 0 9 8 7 6	8 0 8 7 7 6
157420.8205	-6.4011	3	21.0046	15	306	9 0 9 9 8 7	8 0 8 8 8 7
157420.8206	-5.5182	3	21.0046	17	306	9 0 9 10 9 8	8 0 8 9 9 8
157420.8207	-6.9916	3	21.0046	17	306	9 0 9 8 9 8	8 0 8 9 9 8
157420.8217	-5.2436	3	21.0046	15	306	9 0 9 8 8 7	8 0 8 8 8 7
157420.8218	-5.5115	3	21.0046	17	306	9 0 9 8 9 8	8 0 8 8 9 8
157420.8219	-6.5068	3	21.0046	13	306	9 0 9 8 7 6	8 0 8 8 7 6
157420.8225	-6.7276	3	21.0046	21	306	9 0 9 9 10 10	8 0 8 9 9 9
157420.8232	-5.6117	3	21.0046	19	306	9 0 9 9 8 9	8 0 8 9 8 9
157420.8233	-5.3473	3	21.0046	23	306	9 0 9 9 10 11	8 0 8 9 10 11
157420.8234	-3.6051	3	21.0046	21	306	9 0 9 10 10 10	8 0 8 9 9 9
157420.8235	-3.5646	3	21.0046	23	306	9 0 9 10 11 11	8 0 8 9 10 10
157420.8236	-6.7823	3	21.0046	19	306	9 0 9 8 9 9	8 0 8 9 8 8
157420.8242	-5.6052	3	21.0046	19	306	9 0 9 8 8 9	8 0 8 7 8 9
157420.8243	-5.3469	3	21.0046	21	306	9 0 9 9 9 10	8 0 8 8 9 10
157420.8244	-6.9486	3	21.0046	21	306	9 0 9 10 10 10	8 0 8 8 9 9
157420.8246	-6.7637	3	21.0046	17	306	9 0 9 8 8 8	8 0 8 8 7 7
157420.8268	-6.7472	3	21.0046	23	306	9 0 9 9 10 11	8 0 8 9 9 10
157420.8272	-5.2873	3	21.0046	15	306	9 0 9 8 7 7	8 0 8 7 7 7
157420.8273	-5.5730	3	21.0046	19	306	9 0 9 10 9 9	8 0 8 9 9 9
157420.8277	-3.5601	3	21.0046	23	306	9 0 9 10 10 11	8 0 8 9 9 10
157420.8278	-3.5229	3	21.0046	25	306	9 0 9 10 11 12	8 0 8 9 10 11
157420.8283	-5.3020	3	21.0046	17	306	9 0 9 8 8 8	8 0 8 8 8 8
157420.8284	-5.5673	3	21.0046	19	306	9 0 9 8 9 9	8 0 8 8 9 9
157420.8287	-6.9533	3	21.0046	23	306	9 0 9 10 10 11	8 0 8 8 9 10
157420.8288	-6.7706	3	21.0046	19	306	9 0 9 8 8 9	8 0 8 8 7 8
157420.8316	-5.3340	3	21.0046	17	306	9 0 9 8 7 8	8 0 8 7 7 8
157420.8327	-5.3470	3	21.0046	19	306	9 0 9 8 8 9	8 0 8 8 8 9
157420.8328	-6.4190	3	21.0046	17	306	9 0 9 8 7 8	8 0 8 8 7 8
157421.7319	-5.5729	3	21.0046	17	306	9 0 9 9 9 8	8 0 8 8 8 8
157421.7320	-5.5090	3	21.0046	19	306	9 0 9 10 10 9	8 0 8 9 9 9
157421.7321	-5.4694	3	21.0046	21	306	9 0 9 10 11 10	8 0 8 9 10 10
174909.0780	-5.4466	3	26.2556	25	306	10 0 10 11 12 12	9 0 9 10 11 12
174909.0781	-5.4943	3	26.2556	23	306	10 0 10 10 11 11	9 0 9 9 10 11
174909.8854	-5.4858	3	26.2556	17	306	10 0 10 10 9 8	9 0 9 10 9 8
174909.8855	-5.2156	3	26.2556	21	306	10 0 10 10 11 10	9 0 9 10 11 10
174909.8865	-5.2166	3	26.2556	19	306	10 0 10 10 10 9	9 0 9 9 10 9
174909.8887	-6.9196	3	26.2556	17	306	10 0 10 10 9 8	9 0 9 8 8 7
174909.8889	-6.6455	3	26.2556	21	306	10 0 10 10 11 10	9 0 9 10 10 9
174909.8898	-3.6308	3	26.2556	17	306	10 0 10 9 9 8	9 0 9 8 8 7
174909.8899	-3.5223	3	26.2556	21	306	10 0 10 11 11 10	9 0 9 10 10 9
174909.8900	-3.4817	3	26.2556	23	306	10 0 10 11 12 11	9 0 9 10 11 10
174909.8908	-5.5323	3	26.2556	19	306	10 0 10 10 9 9	9 0 9 10 9 9
174909.8909	-5.2679	3	26.2556	23	306	10 0 10 10 11 11	9 0 9 10 11 11
174909.8910	-6.8662	3	26.2556	21	306	10 0 10 11 11 10	9 0 9 9 10 9
174909.8911	-6.6800	3	26.2556	17	306	10 0 10 9 9 8	9 0 9 9 8 7
174909.8918	-5.2678	3	26.2556	21	306	10 0 10 10 10 10	9 0 9 9 10 10
174909.8937	-5.2031	3	26.2556	15	306	10 0 10 9 8 7	9 0 9 8 8 7
174909.8938	-5.4889	3	26.2556	19	306	10 0 10 11 10 9	9 0 9 10 10 9
174909.8939	-6.9566	3	26.2556	19	306	10 0 10 9 10 9	9 0 9 10 10 9

174909.8941	-6.9145	3	26.2556	19	306	10 0 10 10 9 9	9 0 9 8 8 8
174909.8943	-5.3145	3	26.2556	25	306	10 0 10 10 11 12	9 0 9 10 11 12
174909.8949	-5.2174	3	26.2556	17	306	10 0 10 9 9 8	9 0 9 9 9 8
174909.8950	-5.4829	3	26.2556	19	306	10 0 10 9 10 9	9 0 9 9 10 9
174909.8952	-3.4822	3	26.2556	23	306	10 0 10 11 11 11	9 0 9 10 10 10
174909.8953	-3.4451	3	26.2556	25	306	10 0 10 11 12 12	9 0 9 10 11 11
174909.8962	-6.8747	3	26.2556	23	306	10 0 10 11 11 11	9 0 9 9 10 10
174909.8963	-6.6939	3	26.2556	19	306	10 0 10 9 9 9	9 0 9 9 8 8
174909.8977	-6.9138	3	26.2556	21	306	10 0 10 10 9 10	9 0 9 8 8 9
174909.8979	-6.6926	3	26.2556	25	306	10 0 10 10 11 12	9 0 9 10 10 11
174909.8987	-6.8427	3	26.2556	23	306	10 0 10 11 10 11	9 0 9 8 9 10
174909.8988	-3.4073	3	26.2556	27	306	10 0 10 11 12 13	9 0 9 10 11 12
174909.8989	-6.8421	3	26.2556	23	306	10 0 10 9 10 11	9 0 9 10 9 10
174909.8990	-5.2575	3	26.2556	17	306	10 0 10 9 8 8	9 0 9 8 8 8
174909.8991	-5.5375	3	26.2556	21	306	10 0 10 11 10 10	9 0 9 10 10 10
174909.8997	-6.8872	3	26.2556	25	306	10 0 10 11 11 12	9 0 9 9 10 11
174909.8998	-6.7075	3	26.2556	21	306	10 0 10 9 9 10	9 0 9 9 8 9
174909.9001	-5.2709	3	26.2556	19	306	10 0 10 9 9 9	9 0 9 9 9 9
174909.9002	-6.3415	3	26.2556	17	306	10 0 10 9 8 8	9 0 9 9 8 8
174909.9027	-5.3010	3	26.2556	19	306	10 0 10 9 8	9 0 9 8 8 9
174909.9037	-5.3131	3	26.2556	21	306	10 0 10 9 9 10	9 0 9 9 9 10
174909.9038	-6.3087	3	26.2556	19	306	10 0 10 9 8 9	9 0 9 9 8 9
174910.7984	-5.5340	3	26.2556	19	306	10 0 10 10 10 9	9 0 9 9 9 9
174910.7986	-5.4421	3	26.2556	23	306	10 0 10 11 12 11	9 0 9 10 11 11
192397.4734	-5.4231	3	32.0899	27	306	11 0 11 12 13 13	10 0 10 11 12 13
192397.4735	-5.5025	3	32.0899	23	306	11 0 11 11 11 11	10 0 10 10 10 11
192398.2853	-5.4613	3	32.0900	19	306	11 0 11 11 10 9	10 0 10 11 10 9
192398.2854	-5.1969	3	32.0900	23	306	11 0 11 11 12 11	10 0 10 11 12 11
192398.2863	-6.1365	3	32.0900	23	306	11 0 11 12 12 11	10 0 10 11 12 11
192398.2864	-5.1966	3	32.0900	21	306	11 0 11 11 11 10	10 0 10 10 11 10
192398.2887	-6.8415	3	32.0900	19	306	11 0 11 11 10 9	10 0 10 9 9 8
192398.2889	-6.5968	3	32.0900	23	306	11 0 11 11 12 11	10 0 10 11 11 10
192398.2897	-5.5030	3	32.0899	21	306	11 0 11 11 10 10	10 0 10 11 10 10
192398.2898	-3.4571	3	32.0900	21	306	11 0 11 11 11 10	10 0 10 10 10 9
192398.2899	-3.3727	3	32.0900	25	306	11 0 11 12 13 12	10 0 10 11 12 11
192398.2900	-6.7002	3	32.0900	21	306	11 0 11 10 11 10	10 0 10 11 10 9
192398.2906	-5.2437	3	32.0899	23	306	11 0 11 11 11 11	10 0 10 10 11 11
192398.2908	-6.8029	3	32.0900	23	306	11 0 11 12 12 11	10 0 10 10 11 10
192398.2910	-6.6206	3	32.0900	19	306	11 0 11 10 10 9	10 0 10 10 9 8
192398.2926	-5.5400	3	32.0899	23	306	11 0 11 11 10 11	10 0 10 11 10 11
192398.2927	-5.2881	3	32.0899	27	306	11 0 11 11 12 13	10 0 10 11 12 13
192398.2931	-6.8465	3	32.0899	21	306	11 0 11 11 10 10	10 0 10 9 9 9
192398.2933	-6.6233	3	32.0899	25	306	11 0 11 11 12 12	10 0 10 11 11 11
192398.2935	-5.5348	3	32.0899	23	306	11 0 11 10 10 11	10 0 10 9 10 11
192398.2936	-5.2861	3	32.0899	25	306	11 0 11 11 11 12	10 0 10 10 11 12
192398.2937	-5.1840	3	32.0900	17	306	11 0 11 10 9 8	10 0 10 9 9 8
192398.2938	-5.4641	3	32.0900	21	306	11 0 11 12 11 10	10 0 10 11 11 10
192398.2939	-6.9349	3	32.0900	21	306	11 0 11 10 11 10	10 0 10 11 11 10
192398.2941	-3.4158	3	32.0899	23	306	11 0 11 11 11 11	10 0 10 10 10 10
192398.2942	-3.3390	3	32.0899	27	306	11 0 11 12 13 13	10 0 10 11 12 12
192398.2948	-5.1970	3	32.0900	19	306	11 0 11 10 10 9	10 0 10 10 10 9
192398.2949	-6.2688	3	32.0900	17	306	11 0 11 10 9 8	10 0 10 10 9 8
192398.2951	-6.8181	3	32.0899	25	306	11 0 11 12 12 12	10 0 10 10 11 11
192398.2952	-6.6404	3	32.0899	21	306	11 0 11 10 10 10	10 0 10 10 9 9
192398.2962	-6.8540	3	32.0899	23	306	11 0 11 11 10 11	10 0 10 9 9 10
192398.2963	-6.6514	3	32.0899	27	306	11 0 11 11 12 13	10 0 10 11 11 12
192398.2971	-3.3748	3	32.0899	25	306	11 0 11 11 11 12	10 0 10 10 10 11
192398.2972	-3.3043	3	32.0899	29	306	11 0 11 12 13 14	10 0 10 11 12 13

192398.2980	-5.2339	3	32.0899	19	306	11 0 11 10 9 9	10 0 10 9 9 9
192398.2981	-5.5077	3	32.0899	23	306	11 0 11 12 11 11	10 0 10 11 11 11
192398.2990	-5.2464	3	32.0899	21	306	11 0 11 10 10 10	10 0 10 10 10 10
192398.2991	-6.2408	3	32.0899	19	306	11 0 11 10 9 9	10 0 10 10 9 9
192398.3011	-5.2746	3	32.0899	21	306	11 0 11 10 9 10	10 0 10 9 9 10
192398.3020	-5.2859	3	32.0899	23	306	11 0 11 10 10 11	10 0 10 10 10 11
192398.3021	-5.5372	3	32.0899	25	306	11 0 11 10 11 12	10 0 10 10 11 12
192399.1930	-5.5020	3	32.0899	21	306	11 0 11 11 11 10	10 0 10 10 10 10
192399.1931	-5.4531	3	32.0899	23	306	11 0 11 12 12 11	10 0 10 11 11 11
192399.1932	-5.4193	3	32.0899	25	306	11 0 11 12 13 12	10 0 10 11 12 12
209885.1291	-5.4037	3	38.5077	29	306	12 0 12 13 14 14	11 0 11 12 13 14
209885.1292	-5.4348	3	38.5077	27	306	12 0 12 13 13 13	11 0 11 12 12 13
209885.9448	-5.4408	3	38.5077	21	306	12 0 12 12 11 10	11 0 11 12 11 10
209885.9449	-5.1826	3	38.5077	25	306	12 0 12 12 13 12	11 0 11 12 13 12
209885.9458	-5.1812	3	38.5077	23	306	12 0 12 12 12 11	11 0 11 11 12 11
209885.9483	-6.7822	3	38.5077	21	306	12 0 12 12 11 10	11 0 11 10 10 9
209885.9484	-5.4786	3	38.5076	23	306	12 0 12 12 11 11	11 0 11 12 11 11
209885.9485	-5.2267	3	38.5076	27	306	12 0 12 12 13 13	11 0 11 12 13 13
209885.9493	-3.3523	3	38.5077	23	306	12 0 12 12 12 11	11 0 11 11 11 10
209885.9494	-3.2755	3	38.5077	27	306	12 0 12 13 14 13	11 0 11 12 13 12
209885.9503	-6.7552	3	38.5077	25	306	12 0 12 13 13 12	11 0 11 11 12 11
209885.9504	-6.5760	3	38.5077	21	306	12 0 12 11 11 10	11 0 11 11 10 9
209885.9509	-5.5127	3	38.5077	25	306	12 0 12 12 11 12	11 0 11 12 11 12
209885.9510	-5.2672	3	38.5077	29	306	12 0 12 12 13 14	11 0 11 12 13 14
209885.9518	-5.2648	3	38.5077	27	306	12 0 12 12 12 13	11 0 11 11 12 13
209885.9519	-6.7949	3	38.5076	23	306	12 0 12 12 11 11	11 0 11 10 10 10
209885.9521	-6.5903	3	38.5076	27	306	12 0 12 12 13 13	11 0 11 12 12 12
209885.9529	-3.2761	3	38.5076	27	306	12 0 12 13 13 13	11 0 11 12 12 12
209885.9530	-3.2442	3	38.5076	29	306	12 0 12 13 14 14	11 0 11 12 13 13
209885.9532	-5.1693	3	38.5077	19	306	12 0 12 11 10 9	11 0 11 10 10 9
209885.9533	-5.4432	3	38.5077	23	306	12 0 12 13 12 11	11 0 11 12 12 11
209885.9534	-6.9239	3	38.5077	23	306	12 0 12 11 12 11	11 0 11 12 12 11
209885.9538	-6.7756	3	38.5076	27	306	12 0 12 13 13 13	11 0 11 11 12 12
209885.9539	-6.6004	3	38.5076	23	306	12 0 12 11 11 11	11 0 11 11 10 10
209885.9542	-6.9377	3	38.5077	23	306	12 0 12 13 12 11	11 0 11 11 12 11
209885.9543	-5.1814	3	38.5077	21	306	12 0 12 11 11 10	11 0 11 11 11 10
209885.9545	-6.8089	3	38.5077	25	306	12 0 12 12 11 12	11 0 11 10 10 11
209885.9546	-6.6212	3	38.5077	29	306	12 0 12 12 13 14	11 0 11 12 12 13
209885.9554	-3.3135	3	38.5077	25	306	12 0 12 11 11 12	11 0 11 10 10 11
209885.9555	-3.2122	3	38.5077	31	306	12 0 12 13 14 15	11 0 11 12 13 14
209885.9563	-6.7987	3	38.5077	29	306	12 0 12 13 13 14	11 0 11 11 12 13
209885.9564	-6.6236	3	38.5077	25	306	12 0 12 11 11 12	11 0 11 11 10 11
209885.9568	-5.2156	3	38.5076	21	306	12 0 12 11 10 10	11 0 11 10 10 10
209885.9569	-6.9769	3	38.5076	25	306	12 0 12 11 12 12	11 0 11 12 12 12
209885.9577	-5.2273	3	38.5076	23	306	12 0 12 11 11 11	11 0 11 11 11 11
209885.9578	-5.4783	3	38.5076	25	306	12 0 12 11 12 12	11 0 11 11 12 12
209885.9594	-5.2538	3	38.5077	23	306	12 0 12 11 10 11	11 0 11 10 10 11
209885.9603	-5.2645	3	38.5077	25	306	12 0 12 11 11 12	11 0 11 11 11 12
209886.8483	-5.4319	3	38.5076	25	306	12 0 12 13 13 12	11 0 11 12 12 12
209886.8484	-5.4005	3	38.5076	27	306	12 0 12 13 14 13	11 0 11 12 13 13
227371.9779	-5.3880	3	45.5087	31	306	13 0 13 14 15 15	12 0 12 13 14 15
227372.7976	-5.1700	3	45.5087	25	306	13 0 13 13 13 12	12 0 12 12 13 12
227372.7997	-5.4584	3	45.5087	25	306	13 0 13 13 12 12	12 0 12 13 12 12
227372.7998	-5.2130	3	45.5087	29	306	13 0 13 13 14 14	12 0 12 13 14 14
227372.8002	-6.7382	3	45.5087	23	306	13 0 13 13 12 11	12 0 12 11 11 10
227372.8004	-6.5352	3	45.5087	27	306	13 0 13 13 14 13	12 0 12 13 13 12
227372.8006	-5.2107	3	45.5087	27	306	13 0 13 13 13 13	12 0 12 12 13 13
227372.8012	-3.2202	3	45.5087	27	306	13 0 13 14 14 13	12 0 12 13 13 12

227372.8013	-3.1883	3	45.5087	29	306	13 0 13 14 15 14	12 0 12 13 14 13
227372.8019	-5.2510	3	45.5087	31	306	13 0 13 13 14 15	12 0 12 13 14 15
227372.8021	-6.7203	3	45.5087	27	306	13 0 13 14 14 13	12 0 12 12 13 12
227372.8022	-6.5435	3	45.5087	23	306	13 0 13 12 12 11	12 0 12 12 11 10
227372.8027	-5.2482	3	45.5087	29	306	13 0 13 13 13 14	12 0 12 12 13 14
227372.8033	-6.7567	3	45.5087	25	306	13 0 13 13 12 12	12 0 12 11 11 11
227372.8034	-6.5672	3	45.5087	29	306	13 0 13 13 14 14	12 0 12 13 13 13
227372.8042	-3.1591	3	45.5087	31	306	13 0 13 14 15 15	12 0 12 13 14 14
227372.8043	-6.7987	3	45.5087	27	306	13 0 13 12 13 13	12 0 12 13 12 12
227372.8050	-6.7447	3	45.5087	29	306	13 0 13 14 14 14	12 0 12 12 13 13
227372.8051	-5.1587	3	45.5087	21	306	13 0 13 12 11 10	12 0 12 11 11 10
227372.8052	-5.4259	3	45.5087	25	306	13 0 13 14 13 12	12 0 12 13 13 12
227372.8055	-6.7757	3	45.5087	27	306	13 0 13 13 12 13	12 0 12 11 11 12
227372.8056	-6.6003	3	45.5087	31	306	13 0 13 13 14 15	12 0 12 13 13 14
227372.8061	-5.1700	3	45.5087	23	306	13 0 13 12 12 11	12 0 12 12 12 11
227372.8064	-3.1573	3	45.5087	31	306	13 0 13 14 14 15	12 0 12 13 13 14
227372.8072	-6.7713	3	45.5087	31	306	13 0 13 14 14 15	12 0 12 12 13 14
227372.8073	-6.5982	3	45.5087	27	306	13 0 13 12 12 13	12 0 12 12 11 12
227372.8081	-5.2018	3	45.5087	23	306	13 0 13 12 11 11	12 0 12 11 11 11
227372.8082	-6.9747	3	45.5087	27	306	13 0 13 12 13 13	12 0 12 13 13 13
227372.8090	-5.2128	3	45.5087	25	306	13 0 13 12 12 12	12 0 12 12 12 12
227372.8103	-5.2378	3	45.5087	25	306	13 0 13 12 11 12	12 0 12 11 11 12
227372.8104	-5.4912	3	45.5087	29	306	13 0 13 14 13 14	12 0 12 13 13 14
227372.8112	-5.2479	3	45.5087	27	306	13 0 13 12 12 13	12 0 12 12 12 13
227372.8113	-6.0657	3	45.5087	25	306	13 0 13 12 11 12	12 0 12 12 11 12
227373.6966	-5.3853	3	45.5087	29	306	13 0 13 14 15 14	12 0 12 13 14 14
227373.6967	-5.4506	3	45.5087	25	306	13 0 13 14 13 12	12 0 12 13 12 12
244857.9522	-5.4031	3	53.0930	31	306	14 0 14 15 15 15	13 0 13 14 14 15
244857.9523	-5.4086	3	53.0930	31	306	14 0 14 14 15 15	13 0 13 13 14 15
244858.7737	-5.1648	3	53.0930	29	306	14 0 14 14 15 14	13 0 13 14 15 14
244858.7745	-5.1623	3	53.0930	27	306	14 0 14 14 14 13	13 0 13 13 14 13
244858.7763	-5.2030	3	53.0930	31	306	14 0 14 14 15 15	13 0 13 14 15 15
244858.7771	-5.2004	3	53.0930	29	306	14 0 14 14 14 14	13 0 13 13 14 14
244858.7772	-6.7066	3	53.0930	25	306	14 0 14 14 13 12	13 0 13 12 12 11
244858.7774	-6.5187	3	53.0930	29	306	14 0 14 14 15 14	13 0 13 14 14 13
244858.7781	-5.4714	3	53.0930	29	306	14 0 14 14 13 14	13 0 13 14 13 14
244858.7782	-3.1098	3	53.0930	31	306	14 0 14 15 16 15	13 0 13 14 15 14
244858.7783	-6.7494	3	53.0930	27	306	14 0 14 13 14 13	13 0 13 14 13 12
244858.7789	-5.2358	3	53.0930	31	306	14 0 14 14 14 15	13 0 13 13 14 15
244858.7790	-6.6961	3	53.0930	29	306	14 0 14 15 15 14	13 0 13 13 14 13
244858.7791	-6.5214	3	53.0930	25	306	14 0 14 13 13 12	13 0 13 13 12 11
244858.7798	-6.7299	3	53.0930	27	306	14 0 14 14 13 13	13 0 13 12 12 12
244858.7799	-6.5524	3	53.0930	31	306	14 0 14 14 15 15	13 0 13 14 14 14
244858.7807	-3.1104	3	53.0930	31	306	14 0 14 15 15 15	13 0 13 14 14 14
244858.7808	-3.1133	3	53.0930	31	306	14 0 14 14 15 15	13 0 13 13 14 14
244858.7815	-6.7236	3	53.0930	31	306	14 0 14 15 15 15	13 0 13 13 14 14
244858.7816	-6.5524	3	53.0930	27	306	14 0 14 13 13 13	13 0 13 13 12 12
244858.7818	-6.7524	3	53.0930	29	306	14 0 14 14 13 14	13 0 13 12 12 12
244858.7821	-5.1515	3	53.0930	23	306	14 0 14 13 12 11	13 0 13 12 12 11
244858.7822	-5.4119	3	53.0930	27	306	14 0 14 15 14 13	13 0 13 14 14 13
244858.7826	-3.1113	3	53.0930	31	306	14 0 14 14 14 15	13 0 13 13 13 14
244858.7827	-3.1094	3	53.0930	31	306	14 0 14 13 14 15	13 0 13 12 13 14
244858.7830	-5.1622	3	53.0930	25	306	14 0 14 13 13 12	13 0 13 13 13 12
244858.7831	-5.4076	3	53.0930	27	306	14 0 14 13 14 13	13 0 13 13 14 13
244858.7835	-6.5814	3	53.0930	29	306	14 0 14 13 13 14	13 0 13 13 12 13
244858.7847	-5.1919	3	53.0930	25	306	14 0 14 13 12 12	13 0 13 12 12 12
244858.7855	-5.2023	3	53.0930	27	306	14 0 14 13 13 13	13 0 13 13 13 13
244858.7856	-6.0192	3	53.0930	25	306	14 0 14 13 12 12	13 0 13 13 12 12

244858.7866	-5.2259	3	53.0930	27	306	14 0 14 13 12 13	13 0 13 12 12 13
244858.7875	-5.2355	3	53.0930	29	306	14 0 14 13 13 14	13 0 13 13 13 14
244859.6706	-5.3733	3	53.0930	31	306	14 0 14 15 16 15	13 0 13 14 15 15
262342.9848	-5.4194	3	61.2607	31	306	15 0 15 14 15 15	14 0 14 13 14 15
262342.9849	-5.4247	3	61.2607	31	306	15 0 15 15 15 15	14 0 14 14 14 15
262343.8085	-5.3995	3	61.2607	27	306	15 0 15 15 14 13	14 0 14 15 14 13
262343.8086	-5.1606	3	61.2607	31	306	15 0 15 15 16 15	14 0 14 15 16 15
262343.8093	-5.8985	3	61.2607	31	306	15 0 15 16 16 15	14 0 14 15 16 15
262343.8094	-5.1578	3	61.2607	29	306	15 0 15 15 15 14	14 0 14 14 15 14
262343.8107	-5.4290	3	61.2606	29	306	15 0 15 15 14 14	14 0 14 15 14 14
262343.8108	-5.9266	3	61.2606	31	306	15 0 15 15 15 15	14 0 14 15 15 15
262343.8115	-5.4250	3	61.2606	29	306	15 0 15 14 14 14	14 0 14 13 14 14
262343.8116	-5.1936	3	61.2606	31	306	15 0 15 15 15 15	14 0 14 14 15 15
262343.8121	-6.6855	3	61.2607	27	306	15 0 15 15 14 13	14 0 14 13 13 12
262343.8122	-6.5098	3	61.2607	31	306	15 0 15 15 16 15	14 0 14 15 15 14
262343.8124	-5.4565	3	61.2607	31	306	15 0 15 15 14 15	14 0 14 15 14 15
262343.8130	-3.0669	3	61.2607	31	306	15 0 15 16 16 15	14 0 14 15 15 14
262343.8131	-3.0699	3	61.2607	31	306	15 0 15 15 16 15	14 0 14 14 15 14
262343.8132	-5.4526	3	61.2607	31	306	15 0 15 14 14 15	14 0 14 13 14 15
262343.8139	-6.5080	3	61.2607	27	306	15 0 15 14 14 13	14 0 14 14 13 12
262343.8144	-6.7120	3	61.2606	29	306	15 0 15 15 14 14	14 0 14 13 13 13
262343.8152	-3.0681	3	61.2606	31	306	15 0 15 14 15 15	14 0 14 13 14 14
262343.8153	-6.8424	3	61.2606	31	306	15 0 15 14 15 15	14 0 14 15 14 14
262343.8161	-6.5410	3	61.2606	29	306	15 0 15 14 14 14	14 0 14 14 13 13
262343.8169	-3.0666	3	61.2607	31	306	15 0 15 15 14 15	14 0 14 14 13 14
262343.8170	-5.1475	3	61.2607	25	306	15 0 15 14 13 12	14 0 14 13 13 12
262343.8171	-6.9357	3	61.2607	29	306	15 0 15 14 15 14	14 0 14 15 15 14
262343.8177	-6.5721	3	61.2607	31	306	15 0 15 14 14 15	14 0 14 14 13 14
262343.8178	-6.9458	3	61.2607	29	306	15 0 15 16 15 14	14 0 14 14 15 14
262343.8179	-5.1577	3	61.2607	27	306	15 0 15 14 14 13	14 0 14 14 14 13
262343.8192	-5.1855	3	61.2606	27	306	15 0 15 14 13 13	14 0 14 13 13 13
262343.8200	-5.1953	3	61.2606	29	306	15 0 15 14 14 14	14 0 14 14 14 14
262343.8209	-5.2177	3	61.2607	29	306	15 0 15 14 13 14	14 0 14 13 13 14
262343.8217	-5.2268	3	61.2607	31	306	15 0 15 14 14 15	14 0 14 14 14 15
262344.7029	-5.3902	3	61.2606	31	306	15 0 15 16 16 15	14 0 14 15 15 15
279827.0083	-5.4374	3	70.0115	31	306	16 0 16 16 15 15	15 0 15 15 14 15
279827.8340	-5.3917	3	70.0115	29	306	16 0 16 16 15 14	15 0 15 16 15 14
279827.8348	-5.1562	3	70.0115	31	306	16 0 16 16 16 15	15 0 15 15 16 15
279827.8359	-5.4192	3	70.0115	31	306	16 0 16 16 15 15	15 0 15 16 15 15
279827.8367	-5.4154	3	70.0115	31	306	16 0 16 15 15 15	15 0 15 14 15 15
279827.8376	-6.6730	3	70.0115	29	306	16 0 16 16 15 14	15 0 15 14 14 13
279827.8385	-3.0299	3	70.0115	31	306	16 0 16 15 16 15	15 0 15 14 15 14
279827.8394	-6.5020	3	70.0115	29	306	16 0 16 15 15 14	15 0 15 15 14 13
279827.8396	-6.7026	3	70.0115	31	306	16 0 16 16 15 15	15 0 15 14 14 14
279827.8404	-3.0302	3	70.0115	31	306	16 0 16 16 15 15	15 0 15 15 14 14
279827.8412	-6.5369	3	70.0115	31	306	16 0 16 15 15 15	15 0 15 15 14 14
279827.8419	-3.0294	3	70.0115	31	306	16 0 16 15 14 15	15 0 15 14 13 14
279827.8425	-5.1464	3	70.0115	27	306	16 0 16 15 14 13	15 0 15 14 14 13
279827.8433	-5.1560	3	70.0115	29	306	16 0 16 15 15 14	15 0 15 15 15 14
279827.8452	-5.1915	3	70.0115	31	306	16 0 16 15 15 15	15 0 15 15 15 15
279827.8459	-5.2128	3	70.0115	31	306	16 0 16 15 14 15	15 0 15 14 14 15
279827.8467	-5.9128	3	70.0115	31	306	16 0 16 15 14 15	15 0 15 15 14 15
279828.7261	-5.4133	3	70.0115	31	306	16 0 16 16 16 15	15 0 15 15 15 15
279828.7262	-5.4113	3	70.0115	31	306	16 0 16 15 16 15	15 0 15 14 15 15
297309.9554	-5.4562	3	79.3456	31	306	17 0 17 16 15 15	16 0 16 15 14 15
297310.7828	-5.3866	3	79.3456	31	306	17 0 17 17 16 15	16 0 16 17 16 15
297310.7835	-5.3827	3	79.3456	31	306	17 0 17 16 16 15	16 0 16 15 16 15
297310.7864	-6.6681	3	79.3456	31	306	17 0 17 17 16 15	16 0 16 15 15 14

297310.7873	-2.9968	3	79.3456	31	306	17 0 17 17 16 15	16 0 16 16 15 14
297310.7881	-6.5024	3	79.3456	31	306	17 0 17 16 16 15	16 0 16 16 15 14
297310.7889	-2.9976	3	79.3455	31	306	17 0 17 16 15 15	16 0 16 15 14 14
297310.7912	-5.1479	3	79.3456	29	306	17 0 17 16 15 14	16 0 16 15 15 14
297310.7921	-5.1570	3	79.3456	31	306	17 0 17 16 16 15	16 0 16 16 16 15
297310.7929	-5.1817	3	79.3455	31	306	17 0 17 16 15 15	16 0 16 15 15 15
297310.7937	-5.8814	3	79.3455	31	306	17 0 17 16 15 15	16 0 16 16 15 15
297311.6730	-5.4305	3	79.3455	31	306	17 0 17 17 16 15	16 0 16 16 15 15
297311.6731	-5.4353	3	79.3455	31	306	17 0 17 16 16 15	16 0 16 15 15 15
314792.5921	-2.9684	3	89.2628	31	306	18 0 18 17 16 15	17 0 17 16 15 14
314792.5961	-5.1518	3	89.2628	31	306	18 0 18 17 16 15	17 0 17 16 16 15
314792.5969	-5.8518	3	89.2628	31	306	18 0 18 17 16 15	17 0 17 17 16 15
314793.4762	-5.4538	3	89.2627	31	306	18 0 18 17 16 15	17 0 17 16 15 15